Construction of a femtosecond pump-probe spectroscopy system and experiments on the photochemistry of 1-diazo-indan-2-one derivatives

Inauguraldissertation

zur
Erlangung der Würde eines Doktors der Philosophie
vorgelegt der
Philosophisch-Naturwissenschaftlichen Fakultät
der Universität Basel

von

Martin Gáplovský

aus Bratislava (Slowakei)

Bratislava, 2006

Genehmigt von der Philosophischen-Naturwissenschaftlichen Fakultät der Universität Basel auf Antrag der Herren

Prof. Dr. Hans-Jakob Wirz

Prof. Dr. Wolf-Dietrich Woggon

Basel, den 18. November 2004

Prof. Dr. Hans-Jakob Wirz
(Dekan)

The work presented here was initiated and supervised by Prof. Dr. Hans-Jakob Wirz at the Chemistry Department of the University of Basel, during the time period from July 2001 to November 2004.

I wish to thank:

- Prof. Dr. Hans-Jakob Wirz for the opportunity to study in his group in Basel, for his kind supervision, remarkable patience and plenty of useful leads and ideas.
- Prof. Dr. Wolf-Dietrich Woggon for co-referring my thesis and interesting collaboration

Table of contents

INTRODUCTION 6

1. CONSTRUCTION OF ULTRA FAST TRANSIENT ABSORPTION SPECTROSCOPY SETUP 8

1.1. FEMTOSECOND LASER SYSTEM 8
1.2. NONCOLLINEAR OPTICAL PARAMETRIC AMPLIFIER – NOPA 11
1.3 OTHER PARTS OF THE PUMP PROBE SETUP 12
1.3.1 DIODE ARRAY SENSOR HAMAMATSU S3094-512Q AND ITS DRIVER CIRCUIT C7884 12
1.3.2 DIGITAL DELAY / PULSE GENERATOR SRS DG535 13
1.3.3 STEPPING MOTOR AND ITS CONTROLLER. 13
1.3.4 DATA ACQUISITION PART 14
1.3.5 USB2000 FIBER OPTIC SPECTROMETER 14
1.3.6 OPTICAL CHOPPER NEW FOCUS MODEL 3501 15
1.3.7 OTHER PARTS 15
1.4. ARRANGEMENT OF THE SETUP 16
1.4.1 THE PRINCIPLE OF THE EXPERIMENT: 16
1.4.2 SYNCHRONIZATION 18
1.4.3 ACQUISITION SOFTWARE 19
1.5. CHARACTERISTICS OF THE SETUP 22
REFERENCES 27

2. PHOTOCHEMISTRY OF 3-DIAZO-2-OXINDOLINE 28

2.1. INTRODUCTION 28
2.1.1 CARBENES 28
2.1.2 PHOTOCHEMISTRY OF α - DIAZO KETONES 30
2.1.3 PHOTOCHEMISTRY OF 1-DIAZO-2-INDANONE AND SIMILAR DERIVATIVES. 34
REFERENCES 37
2.2. PUMP - PROBE EXPERIMENTS 39
2.2.1 DISCUSSION 42
REFERENCES 47

2.3. NANOSECOND LASER FLASH PHOTOLYSIS. **48**
2.3.1 DISCUSSION 51
REFERENCES 57
2.4. CALCULATIONS. **58**
2.4.1 THEORETICAL PROCEDURES 58
2.4.2 RESULTS AND DISCUSSION 59
REFERENCES 64
2.5. INFRA RED SPECTROSCOPY - STEP SCAN EXPERIMENTS **65**
2.5.1 RESULTS AND DISCUSSION 66
REFERENCES 69

3. SUMMARY **70**

4. CURRICULUM VITAE **73**

5. APPENDIX **74**

Introduction

When a chemical reaction occurs, it is relatively rare for it to take place in a single step. Full understanding of a chemical reaction requires the identity and nature of intermediates formed to be determined and knowledge of the processes of bond making and breaking to be established. Even though all the intermediates are by definition reactive species, those of them that are instable under 'normal' conditions so that they can not be isolated are referred to as reactive intermediates. Another simple definition says that the reactive intermediate corresponds to a shallow dip in a diagram of free energy versus reaction coordinate. The chemistry of reactive intermediates has evolved from product driven enterprise, in which the primary information was the analysis of reaction products followed by the deduction of probable mechanism and intermediate[1]. With advances in modern chemical techniques, especially in time resolved spectroscopy, direct observation of the intermediates is more common. In other words, chemist can now look at the beasts themselves, rather than make inferences based upon their footprints. An early triumph of time-resolved spectroscopy was the demonstration (by cine photography) that all four legs of a horse leave the ground when it gallops. Modem techniques using ultra-fast lasers enable processes a many orders of magnitude faster than this to be measured[2].

The detection of changes in the absorbance of reactants or products is a very effective way for monitoring of reaction rates. Study of the fast molecular events requires probing of the system at the time scale of a followed process. The problem is that even the fastest detectors have their time resolution limits given by the nature of the processes they are based on. For measurement of very fast relaxation processes that demand a time resolution below 10^{-10} s most detectors are not fast enough. Here the pump probe technique is the best choice[3]. Central to the pump probe technique is the use of two pulses originating from the same laser source, which is used both to initiate the photochemical or photo physical process with the pump pulse and to examine the subsequent changes in the sample with the probe pulse. Pico- or femto- second time resolution is obtained by sending one of the beams through a motor-driven optical delay

line. Pump beam initiates some process of interest, for example, a chemical reaction. The probe beam, entering the sample later, will be amplified, attenuated, or refracted because of the changes taking place in the sample. Nowadays there exist many variations of this scheme and a large number of experimental examples is in use[4,5,6]. UV/VIS and more recently IR and electron transient spectroscopy as well as fluorescence upconversion setups are based on the pump probe technique. One of its useful modifications is the use of a white light (continuum) pulse for probing. This allows to measure entire spectra at a given delay rather than a kinetic trace at a single wavelength as in classical arrangements. In addition, short-pulsed optical parametric amplifiers[7] or oscillators have been realized to be used to provide tunable pump beams. Their wide tuning range allows more detailed investigation compared to restricted use of fixed frequency lasers.

The aim of this thesis is to describe the construction and characteristic of a setup for recording of absorption spectra with a time resolution in the femtosecond time domain. In addition, new experimental results on the photochemistry of 3-diazo-2-indolinone are presented. These investigations are part of a larger project dealing with the photochemistry of 1-diazo-2-indanone derivatives. Besides the pump probe technique, other method were applied, namely time resolved infrared spectroscopy, laser flash photolysis and computational methods.

(1) R.A. Moss, M. S. Platz., M. Jones, Jr. (**2003**). Reactive Intermediate Chemistry. New York, Wiley.

(2) J.D. Simon, Rev. Sci. Instrum. 60 (12), 3597-3624 (**1989**).

(3) Demtröder, W. (**2003**). Laser spectroscopy. Berlin, Springer.

(4) Van Hecke, G. R. (**1998**). A guide to lasers in chemistry. Boston, Jones and Bartlett Publishers.

(5) Andrews, D. L. (**1997**). Lasers in chemistry. Berlin, Springer.

(6) G.D. REID, K. WYNNE, "Time-Resolved Spectroscopy," in the "Handbook of Laser Technology," (Institute of Physics Press, **2003**).

(7) T. Wilhelm, J. Piel, and E. Riedle, Optics Letters 22 (19), 1494-1496 (**1997**).

1. Construction of Ultra fast transient absorption spectroscopy setup

In order to investigate primary photochemical processes, high time resolution is essential. The experimental technique described and used in this thesis is transient absorption pump-probe spectroscopy. In such an experiment, a strong pump pulse is used to initiate a reaction and the reaction kinetics is followed by recording the absorbance of a monitoring pulse, as a function of the time delay between the pump and the monitoring pulse.

1.1. Femtosecond laser system

The CPA-2001 Laser System was manufactured by Clark-MXR.Inc and purchased from their dealer Yobin Yvon GmbH, Germany. Our integrated titanium:sapphire amplified laser system consists of the following main components:

SErF (Erbium doped fiber) fiber oscillator
Pulse stretcher
Regenerative amplifier
ORC-1000 frequency-doubled Nd:YAG pump laser
Pulse compressor

The erbium doped fiber ring oscillator, pumped by the cw diode laser, is passively modelocked by polarization selective elements[1,2]. The lasing wavelength of the fiber oscillator is 1.55 μm with a repetition frequency of around 25 MHz, which is the clock frequency of the whole system. The wavelength region, in which the Ti:Sapphire amplifier[3] operates, is 700-900 nm. Therefore, before injecting the pulses from the fiber oscillator into the amplifier they have to be frequency doubled. There is a photodiode in order to monitor the modelocked, frequency doubled pulses from the fiber oscillator

behind the doubling crystal. From the crystal the 25 MHz 775 nm pulses are guided into a grating based pulse stretcher.

This laser provides the so-called seed beam that is later amplified in a Ti:Sapphire amplifier and compressed to give the final CPA 2001 output. In the Ti:Sa crystal the Al^{3+} ions in the crystal lattice of Al_2O_3 are replaced by Ti^{3+} ions at concentrations of approximately 0.1% by weight, thereby acting as impurity. The principles of operation are characteristic of four level laser systems. However, instead of discrete energy levels giving rise to narrow lasing lines, as in for example Nd^{3+}, very closely spaced vibrationally broadened electronic energy states in Ti^{3+} permit tunable emission over a range of wavelengths. The tuning range is typically 650-1200 nm and the maximum power for emission is between 700 and 900 nm[4]. The Ti:Sapphire amplifier must be pumped by an intense light source in order to establish the population inversion necessary for its operation. Frequency-doubled Nd:YAG pump laser is the primary light source of our amplifier.

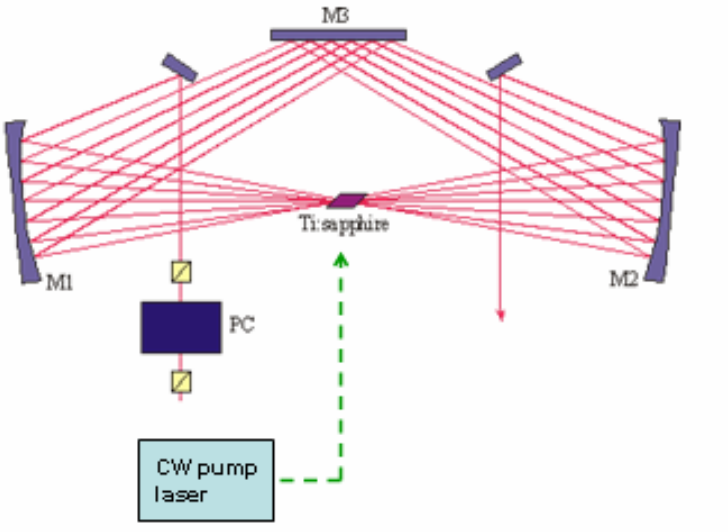

Figure 1: Scheme of Ti:Sa parametric amplifier. The seed beam usually passes crystal several times for stronger amplification.

It raises the Ti:Sa crystal to its excited state to generate a population inversion. As the traveling seed beam passes the Ti:Sa crystal it stimulates the emission depleting the population inversion. In other words, before the excited crystal can lase spontaneously a second laser pulse stimulates the excited population to lase faster than 'normal', on its own wavelength. Since our seed beam is very short, the amplified beam is also very short just stronger. This process takes place several times before the amplified beam proceeds further to the pulse compressor (Figure 1). Logically, pumping has to be somehow synchronized with the amplification. This is achieved by a Pockel's cell. A cell consisting of crystalline material, which exhibits the Pockel's effect, essentially a proportional change in refractive index on application of an electric field. A Pockel's cell is used to rotate the plane of polarization light passing through it or in other words reverse the handedness (90º rotation) of circularly polarized light. Hence, coupling with a polarizer provides an effective shutter action when the voltage is applied, since the polarizer cuts out all the light with rotated plane of polarization. By switching the voltage off the pump beam's path becomes transparent again and amplification of next pulse can take place.

Pulse compression is based on the system of two prisms (Fig 2). Our laser pulse has a relatively broad output wavelength distribution centered around 775 nm as a consequence of the uncertainty principle.

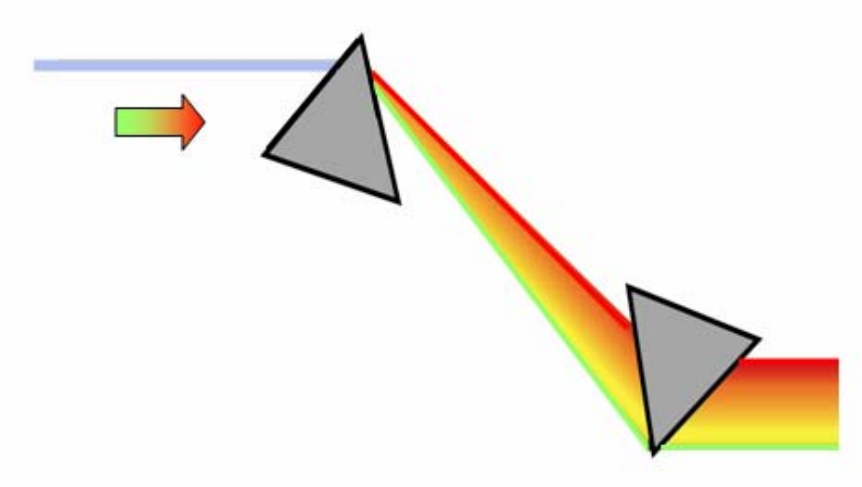

Figure 2: Scheme of a prism pulse compressor.

The wavelengths contained in the initial pulse pass through various optical elements with different velocities and thus take different times to traverse the same distance. The wavelengths whose refractive indexes in the medium are the smallest will traverse the first and vice versa. The result is a chirped pulse, in other words an inhomogeneous distribution of wavelengths separated in time. The compression results from a longer path lengths for the wavelengths that arrive first at the grating and shorter path lengths for those arriving later[5]. In fact, a prism pair provides a wavelength-dependent optical path. By adjusting the prism orientation the path length can be set to make all the travel times closer thus compressing the pulse in time. Effectively, the different wavelengths of the pulse are first separated in space and then compressed even more closely in time and space.

Pulse energy	0.8 mJ at repetition rate 1 kHz.
Pulsewidth (FWHM)	<150 fs
Wavelength	775 nm primary
Repetition Rate	User-adjustable up to 2 kHz
Beam Diameter	4 - 6 mm
Beam Divergence	< 100 microradians
Beam Pointing Stability	< ± μrad/°C

Table 1: Characteristic of CPA 2001 laser system.

1.2. Noncollinear Optical Parametric Amplifier – NOPA

The NOPA plays an important role in the setup. It provides the setup with the pump laser beam of chosen wavelength. The available range is 470-700 nm.

In the NOPA broadband continuum light is amplified in a noncollinearly phase matched parametric amplifier[6,7]. Because of noncollinear geometry, no dichroic mirrors or polarizing optics are needed to separate the signal pulses from the pump and idler pulses (Figure 3).

A seed pulse, which is a single filament of white-light continuum generated in a 1-mm-thick piece of sapphire, is amplified by the frequency-doubled output of a Ti:sapphire amplifier.

Technically, one part of the CPA 2001 output is split into two portions (inside the NOPA box). The more intense one is frequency doubled in the nonlinear optical crystal (β–barium borate BBO in our case) and gives 388 nm pumping beam. The less intensive one is used to produce white light chirped continuum (seed pulse).

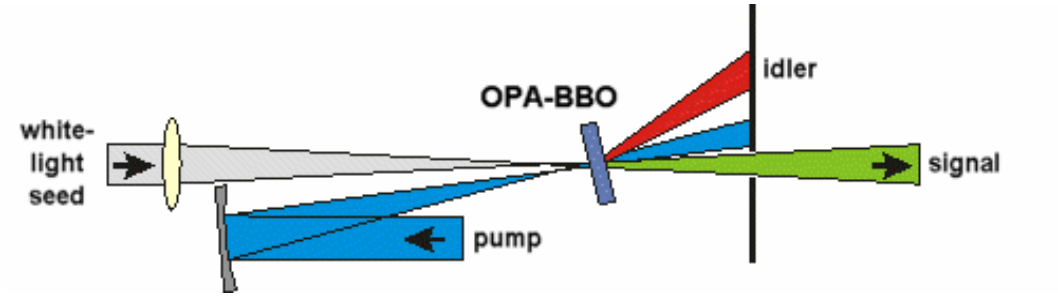

Figure 3: NOPA – noncolinear optical parametric amplifier.

The pump beam focused onto the BBO generates a cone of parametric superfluorescence. By directing the continuum seed beam along the cone axis, a large spectral bandwidth from the white light can be simultaneously phase matched. Adjustment of the relative delay between the pump and the seed beams changes the center wavelength of the amplified light. One big advantage of this scheme is that relatively thick crystals can be employed (typically 2 mm), which results in a high single-pass gain. The amplified output is then recompressed using a prism pair yielding sub-30-fs continuously tunable visible pulses[8].

1.3 Other parts of the Pump Probe setup

1.3.1 Diode array sensor Hamamatsu S3094-512Q and its driver circuit C7884

The self-scanning photodiode array is designed as a detector for multichannel spectroscopy. Its 512 diodes, together with the grating, provide our setup with a

reasonable spectral resolution about 0.75 nm (the continuum ranges from 300 to 690 nm). The sensors have good UV sensitivity and wide dynamic range. They are coupled with their driver circuits - an electronic part responsible for operating the detectors, signal processing and reading out the signal. The highest possible master clock frequency of the circuit is 2 MHz. Since the data video signal readout frequency is ¼ of the clock frequency, operating the sensors on the maximum frequency 2 MHz will provide us with readout time per channel (t) 2 μs. Thus the time required for one scan t_{scan} becomes:

t_{scan} = t x Number of sensors channels (512 in our case).

t_{scan} = 2 μs x 512 = 1024 μs. That is sufficient and corresponds to laser maximum frequency 1 kHz. In fact, the real working frequency is for other reasons about half of the possible maximum.

1.3.2 Digital Delay / Pulse Generator SRS DG535

Proper timing is essential to operate such a complex system like our setup. The primary clock of the setup is the one of the CPA-2001, but different parts have to be triggered with different delays. That is achieved mostly by the DG535 device. It is very accurate (1ppm) and has a low time jitter, about 50ps. The rise time of a generated signal can be as small as 150 ps which makes DG535 especially suitable to be used with a streak camera. It can supply four precisely timed logic transitions synchronized by either external trigger or internal clock and their combinations.

1.3.3 Stepping motor and its controller.

The possibility to adjust the delay between excitation and probing is an inevitable attribute of every pump probe system. Since the delays go usually down to femtoseconds it can be achieved only by varying the optical path of one beam in respect to the other. Moreover, this has to be done very precisely, for example 10 fs delay corresponds to 3

μm difference in optical path. We use a Physik Instrumente translation stage with retroreflecting mirror attached. The stage is operated from the C-500 controlling unit connected to the computer by GPIB port via GPIB/USB interface.

1.3.4 Data acquisition part

The way the data is collected and stored has substantial impact on the performance of the whole setup, especially when working with higher laser frequencies. The amount of data, acquired during an average experiment, is surprisingly high. That is actually the reason why data acquisition and its later processing are performed separately in our system. The analog signal from detectors is converted to the digital one and stored in the memory of UF3120 Transient Recorder. It is a PCI board supplied by Strategic Test Scandinavia AB. It converts analog input signal into 12 bits binary digital words and includes 8 Mega Sample on-board memory. Our version contains two analog input channels and follows maximum sampling rates 10 MS/s per channel. Multiple Recording and Gated Sampling options are also included. The card had to be extended later by additional 8 digital input channels, due to synchronization with the chopper. The on-board memory allows storing (reading in signals from the arrays) 500 acquisitions from both channels, which is then the coaddition limit for one single experimental time step. SBench data acquisition program and NI LabView driver enable relatively easy control of the card functions.

1.3.5 USB2000 fiber optic spectrometer

This miniature spectrometer is a quite versatile tool, especially useful for adjusting the NOPA output wavelength. It is a plug and play device connected to the computer through the USB port. 2048 elements of linear CCD array provides good spectral resolution (down to 0.3 nm depending on the grating and size the of entrance aperture) and reasonable integration time. Light is brought to the spectrometer by 2 meters long optical fiber with a cosine corrector for emission collection attached on the top. OOIBase32 is the spectrometer operating software installed on the computer.

1.3.6 Optical Chopper New Focus model 3501

The working principle of our detection system requires pump beam chopping. In other words, only every second pump pulse is allowed to excite the sample. The non excited probing of sample serves as a background or a reference, similarly to the steady state spectroscopy. The chopper consists of two parts – a programmable control unit and a chopper head with replaceable wheels. Very useful feature of the device is that it can adjust its chopping frequency to even a sub harmonic of externally supplied signal. The instrument can be programmed remotely via GPIB port.

1.3.7 Other parts

Power meter with two detector heads for measuring different energy scales.
Delay box - home made, adjustable, TTL signal delay box.
Computer - DELL workstation.
Oscilloscope - Tektronixs 10MS digital, 4 channel oscilloscope.
Pumps - HNP Mikrosysteme small volume pump.

1.4. Arrangement of the setup

1.4.1 The principle of the experiment:

The principle of the experiment is quite similar to the ordinary steady state UV/VIS measurements with some exceptions. The desired outcome is a differential spectrum of the species contained in the sample at different times after the excitation rather than just ordinary UV/VIS spectrum. Therefore, there is a ΔOD on the x axis instead of an absorbance. That is because we are interested primarily in the transient absorption spectra, which correspond to the absorbance difference between steady state spectrum and spectrum after the excitation of the sample where a small portion of the compound is photo chemically changed to the transient. However, the procedure is a bit more complex because some corrections have to be applied[9]. The intensity fluctuation of the probe beam is compensated by a second, reference signal, recorded simultaneously. It is a 50 % portion of the probe beam refracted by a beam splitter into a second camera.
Another correction is obtained from a special baseline measurement for which the pump is switched off. In our case, it is every second pump pulse, which is omitted.
Thus, altogether 4 signals are recorded in order to get one ΔOD spectrum. These are namely:
I_{S1} - probe intensity after passing the excited sample,
I_{R1} - probe intensity recorded by the second reference camera,
I_{S2} - probe intensity after passing the steady state sample,
I_{R2} - another probe intensity signal recorded by the reference camera.

Typically, several hundred spectra are collected for one time point and then averaged to reduce the statistical noise with the factor $1/n^{1/2}$.
Another useful correction applied is running the experiment at least twice. Once beginning with a position of delay stage corresponding to the maximum time delay and going down with the delay and second time vice versa. This procedure helps to avoid an

error caused by slow changes of the sample, for example a concentration change, and helps to detect some other possible experimental errors.

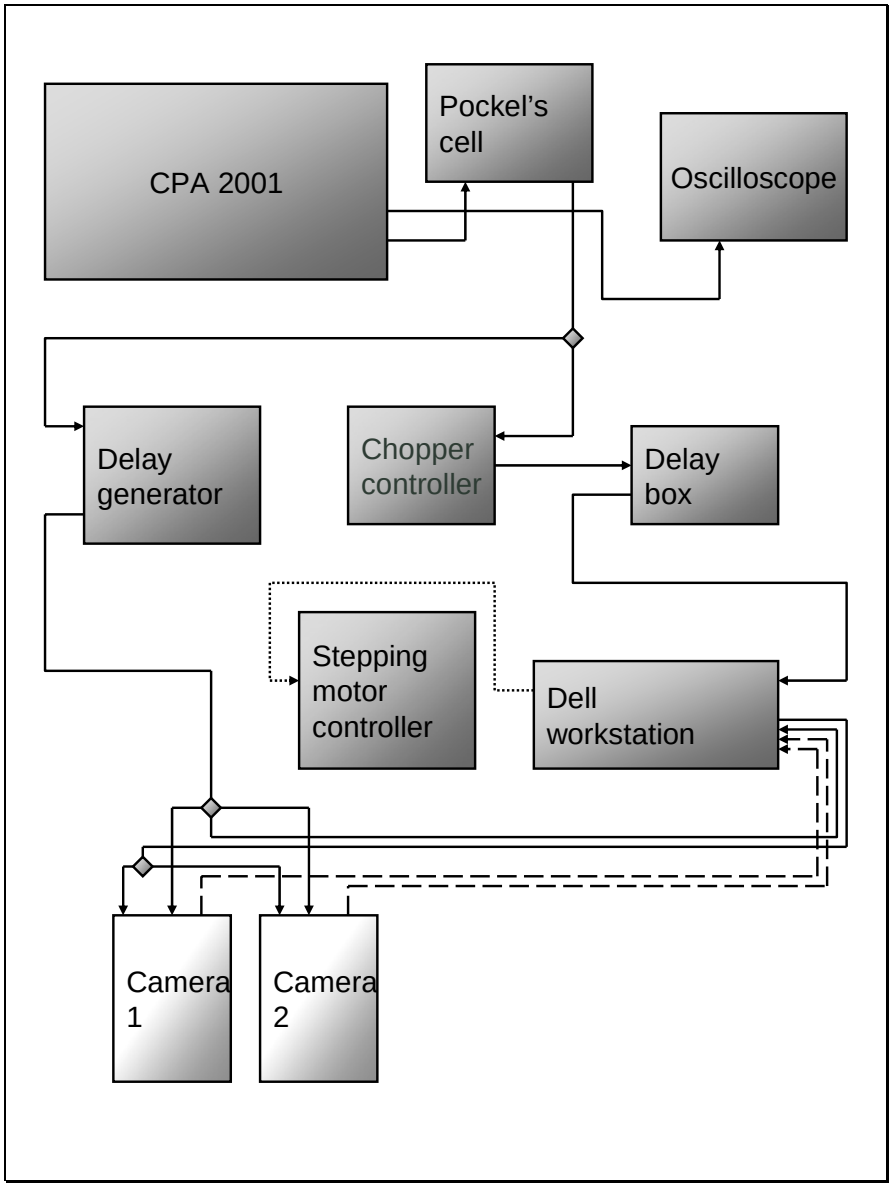

Figure 4: Connection of individual electronic parts – timing, synchronization and data flow. Dotted line represents a USB/GPIB cable, other connections are BNC cables transmitting TTL signals (full lines) and analog signals from detectors (long dash).

In practice the detection looks as following. The continuum pulses, with a energy ~ 0.1 mJ, are imaged onto the sample solution by dispersion-free anastigmatic optics. The pump and probe beams intersect in the sample with an angle of 5°, the probe diameter being 80–100 μm. The sample net thickness is adjustable, however 0.2 mm is the usual value. The fused silica windows (Suprasil I) are 0.16 mm thick. Windows are part of the homemade cell made of a very resistant polymer PEEK (polyaryletheretherketone). The solution is flown out of the interaction region after each laser shot. After an interaction with the sample, the supercontinuum is dispersed by a polychromator to obtain the signal spectrum. It is then registered on a photodiode array with 512 pixels (Hamamatsu). A part of the probe beam is split off before the interaction and is dispersed and registered separately for reference I_R. The differential optical signal ΔOD_{expt} is then obtained as:

$$\Delta OD_{expt} = \frac{1}{n}\sum_{i=1}^{n} \left(\frac{I_{S1}/R_{S1}}{I_{S2}/R_{S2}} - 1\right)$$

1.4.2 Synchronization

Our setup is synchronized with the laser internal clock. The signal is divided in the Pockel's cell RF driver by user-selected factor. The TTL signal taken from the Pockel's cell driver output 2 corresponds with certain delay to the laser pulse of the CPA 2001. Since the time fluctuation is negligible (for our purposes) we do not have to use a special ultra fast diode for synchronization as is usual in many similar setups. The signal with a typical frequency 426 Hz (RF divider set on 40) proceeds subsequently to a delay generator SRS DG535 and the optical chopper driver. SRS DG535 produces another TTL pulse, the START signal for the diode arrays. During the START signal, integration of the light intensity on the photodiodes takes place. The same signal, on the other hand, starts the data readout from sensors to the computer. It is a trigger for the acquisition board. However, the 1MHz clock for diode arrays is independently generated from the acquisition board and is not synchronized with the laser. Fortunately, it does not cause any problems or mismatches when a suitable length of START signal is applied.

The optical chopper has to chop off every second pump pulse for the reasons mentioned above. It adjusts its frequency to one-half that of the trigger signal coming from the pockel's cell driver. The signal coming from the chopper output is fed into the signal divider box which serves basically only to reshape the signal so that it can be read by the digital input channel of our data acquisition computer board. It provides the software with the information whether it is processing an excited or not excited scan. The last signal to be mentioned goes from the computer's USB port through a USB\GPIB interface cable to the delay line controller and back. It is controlled by the software.

1.4.3 Acquisition software

The software used to control the acquisition board to save the data on the disk and to transform them into the final 2D matrix of spectra versus time was written in Labview version 6.3. It is based on a Labview driver with a library of basic commands supplied by the card manufacturer. For data reading the multiple recording option of the acquisition card is used. The scheme of this option is depicted in Figure 5.

Although the DELL workstation we use is a quite powerful computer, it still takes a substantial amount of time to handle the huge amount of data coming from the sensors. 500 co-additions of scans at a certain time delay completely occupy the built-in memory of the card, which is 8 MS. This is the reason why the raw data is first saved on the hard drive and processed only later when the experiment is finished. The data corresponding to each time are written in two separate binary files for each of the two channels (sensors). One file has typically around 8 MB. The A/D signal converter of the card transforms the analog signal into a 12 bit digital one. However, it is stored in the form of 16 bit integers which leaves the upper 4 bits empty or free for the additional digital channels. We use one of them to record signal from the chopper to get the information whether the saved scan corresponds to the excited sample or not. At some point, these 4 upper bits have to be extracted in a process called unmasking.

The data acquisition takes place in the cycles or loops. First, a command is sent to the delay line to move it to the proper position, then the card is restarted, it reads the sensors n times and finally files with the data are saved.

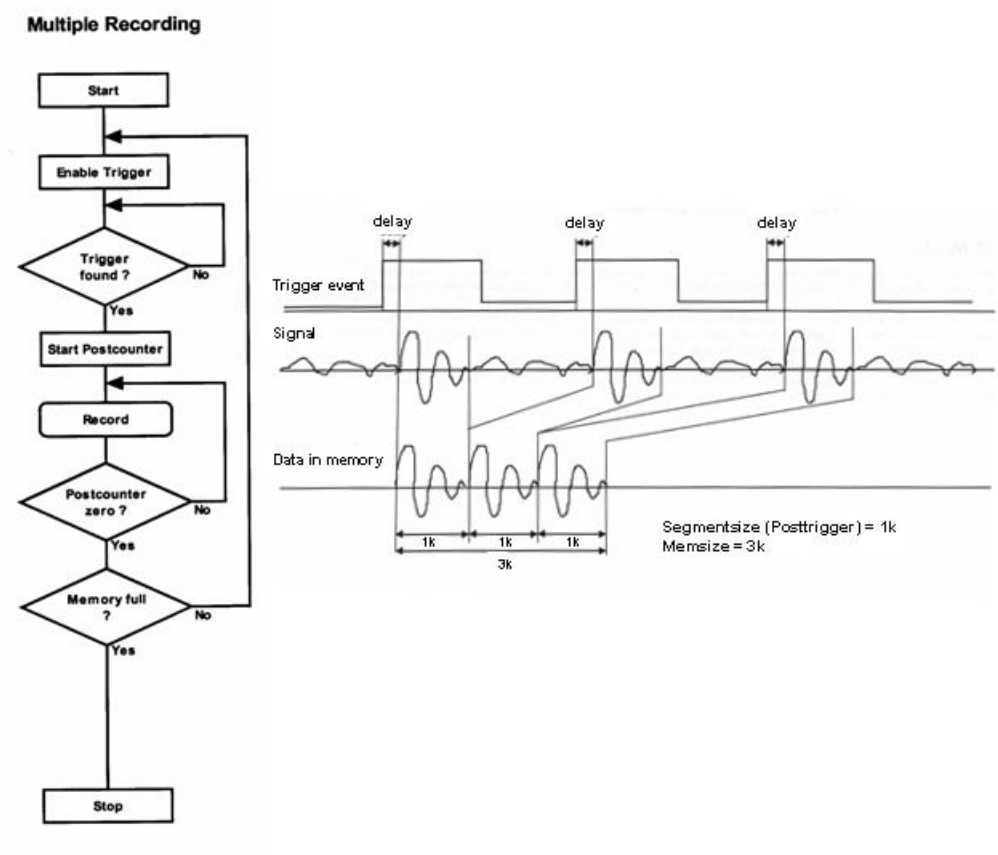

Figure 5: Multiple recording option of the acquisition card. This option uses an onboard trigger re-arming system that allows a high-speed series of waveforms to be recorded without restarting the hardware after each waveform has been processed. The memory of the card is divided into several segments of the same size. In this mode each segment will be automatically filled with data when a trigger event occurs and then the trigger is rearmed for the next event.

The second part of the software (Figure 6) does mainly algebra with the arrays and matrixes described above. The final result is a text file containing a single 2D matrix.

This can easily be processed later in some advanced mathematical or statistical software, for example Origin, Excel or Specfit. We often use home-made applications written in the MatLab environment, too.

One application of the particular importance is SPAN[10]. This ultrafast spectroscopy utility was developed at the Humboldt University in Berlin, Germany to treat experimental pump-probe data. Various methods of chirp and baseline correction, measurement averaging, data smoothing and visualization belong to its useful functions.

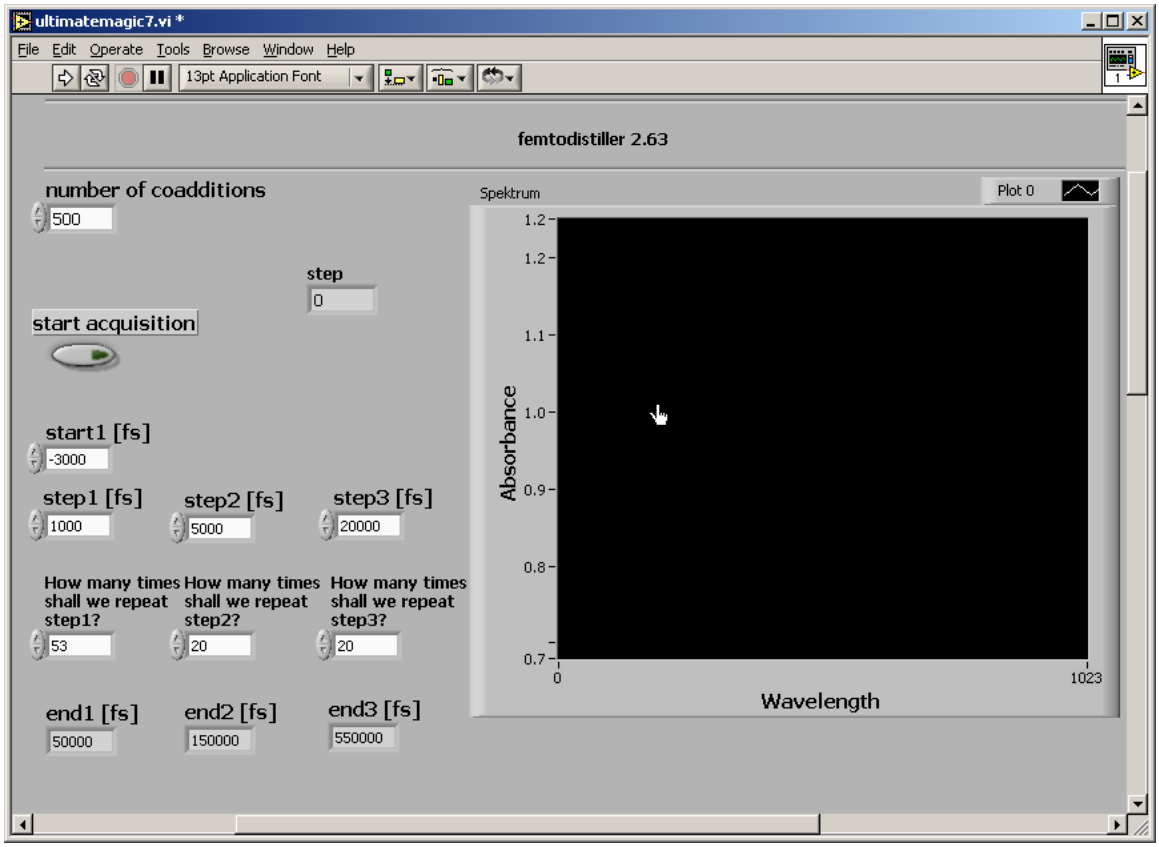

Figure 6: Front panel of a LabView application, which creates a matrix out of raw data saved on a hard drive during the experiment. It recognizes up to three different time steps in one experiment.

In addition to noise reduction achieved by averaging of many scans, the resulting matrix often requires further mathematical treatment such as factor analysis[11]. Factor analysis provides an efficient tool for data reduction and kinetic model selection. It usually leads to a significant elimination of random noise. Another purpose of factor analysis is to determine the number of absorbing species in the reaction system on a model-independent basis. It has some restrictions, however: linearly dependent spectra or essentially parallel concentration profiles will lead to loss of the signal, whereas instrumental instabilities will produce artificial signals. We use most often the factor analysis procedure involved in Specfit or either Matlab or Mathematica applications.

The Specfit[12] software gives us also the possibility to apply global analysis procedures to find a suitable reaction model of our investigated system. Multiwavelength data generally lead to a more accurate determination of the relevant rate constants. The determination of the absorption spectra of the individual species participating in a reaction by global analysis helps to distinguish between different mechanistic models.

1.5. Characteristics of the setup

The time resolution of a femtosecond spectroscopy setup is determined by several factors. However, what matters most are the pulse length and the shape of the pump and the probe when they meet in the sample. It would be quite difficult to imagine an experiment with femtosecond time resolution if excitation takes picoseconds. Some mathematical procedures, like pulse deconvolution, can be applied, of course, but they have their limitations.

The manufacturer indicates the pulse length of the CPA 2001 output beam to be about 140 fs (Table 1). The continuum is likely to be somewhat longer. The NOPA output after the compression and frequency doubling can be as short as 90 fs.

There is a direct method for the measurement of ultra short pulse lengths called auto- or crosscorrelation. This method is based on a similar principle as the pump and probe technique. In an autocorrelator, an incoming beam of pulses is split in two. One beam travels through an optical path with a fixed length, the other through a path that includes

an optical delay line. An optical delay line usually consists of a pair of mirrors or a retro-reflector mounted on a motorized translation stage or even a sine-wave-driven loudspeaker. In such a setup, the spatial position of the mirrors on the translation stage is directly related to the relative time-delay between the two beams of pulses.

Both beams are focused in a nonlinear crystal such as BBO in order to produce second-harmonic radiation. Phasematching[13] in the crystal is used to produce a beam at the second-harmonic frequency in which one photon has been taken from one beam and one from the other[14]. Plotting of this beam intensity against the relative time delay gives us information about the pulse length.

The crosscorrelation signal as a function of time delay is proportional to the shape of the incoming pulses. For example, the autocorrelation of a pair of pulses with a Gaussian envelope keeps a Gaussian shape.

We used a simplified version of an autocorrelation experiment to estimate the time resolution of our setup. Rather than frequency mixing in a BBO crystal we follow a two photon absorption by the solvent. In this process, a molecule absorbs two photons (one comes from the pump and the other from the probe, in our case) at approximately the same time and achieves an excited state that corresponds to the sum of the energy of the incident photons. There does not have to be an intermediate state for the atom to reach before arriving at the final excited state (as if it were moving up two stair steps by stepping one at a time). Instead, the atom is excited to a "virtual state" which need not correspond to any electronic or vibrational energy eigenstate.

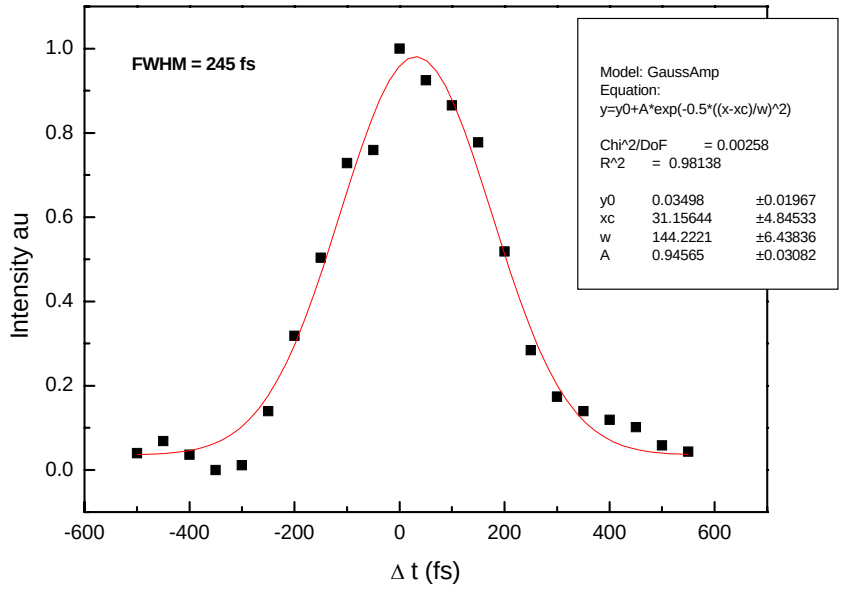

Figure 7: Two-photon absorption in ethyl acetate. Intensity (at one wavelength) of the signal plotted vs. time.

The two-photon absorption measurement in ethyl acetate is shown in Figure 7. The experimental values were fitted by a Gaussian function. The Resulting Full-Width Half-Maximum (FWHM) value 245 fs was multiplied by s factor of 0.71 for Gaussian shaped pulse to obtain an estimate of the pulse length[15].

Besides the pulse length, the probe chirp (spectral distribution in time) and rotational anisotropy[16] affect the femtosecond time resolution. In the case of time chirp a proper mathematical treatment can solve the problem (Figure 8).

The rotational diffusion problem is a consequence of the fact that the laser light is linearly polarized. It is known that a molecule can absorb a photon only if the orientation of its transition dipole matches the polarization of the particular photon.

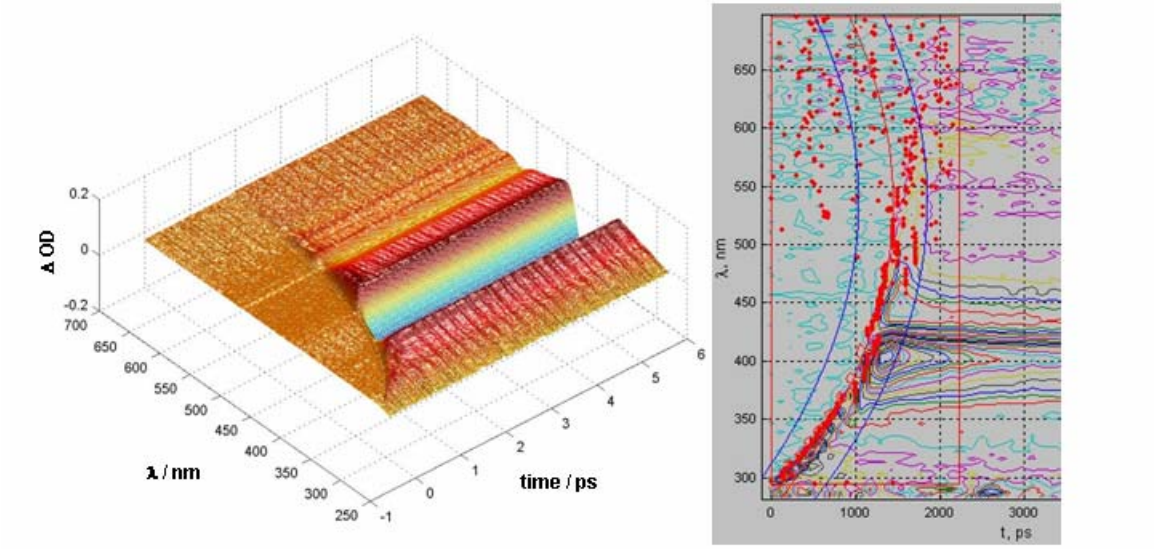

Figure 8: Typical example of chirped 3D spectra (porphyrin molecule) and 2D visualization (SPAN) of the same spectra with 2nd order polynom correction function - red line. The function was fitted to time zero determined from max. d Signal/d Time - red dots.

Therefore, the laser pump beam populates all the excited state molecules with virtually parallel orientation of transition moments. The same holds for probe beam absorption. Since the molecules rotate freely in the solution, the rotational diffusion process influences the evolution of the transient absorbance until the system is equilibrated. For smaller molecules like those we are interested in, the equilibration can take as much as several hundreds of femtoseconds.

To avoid the problem, a magic angle (54.7°) configuration between the pump and the probe polarization should be set. It is usually achieved by using an optical half-wave plate.

We are using a 775 nm light directly from the CPA 2001 to produce the white light continuum. Its typical shape is shown in the Figure 9. The intensity of the white light is sufficient to effectively probe the sample from 300 to 690 nm. In principle, it should be possible to increase the intensity and hence the probing range by compressing the red light pulse, since non-linear optical processes, such as the optical Kerr effect, which is responsible for continuum, are functions of incident light intensity.

Higher intensity of the probe would decrease the noise, too. Unfortunately, it is not feasible to use the whole energy of the red laser beam. An implication of the nonlinear refractive index[17] (optical Kerr effect) is self-focusing or defocusing. As a laser beam is typically more intense in its center, the nonlinear change of the refractive index will be strongest in the center. As a result, the medium will act as an intensity-dependent lens. In white-light generation, self-focusing can result in the beam breaking up into multiple filaments that make the white-light output extremely unstable. It is therefore of the utmost importance to choose the incident power such that white light is generated without producing multiple filaments. For a 100-fs pulse, this usually means that the pulse energy should be limited to approximately 1 μJ.

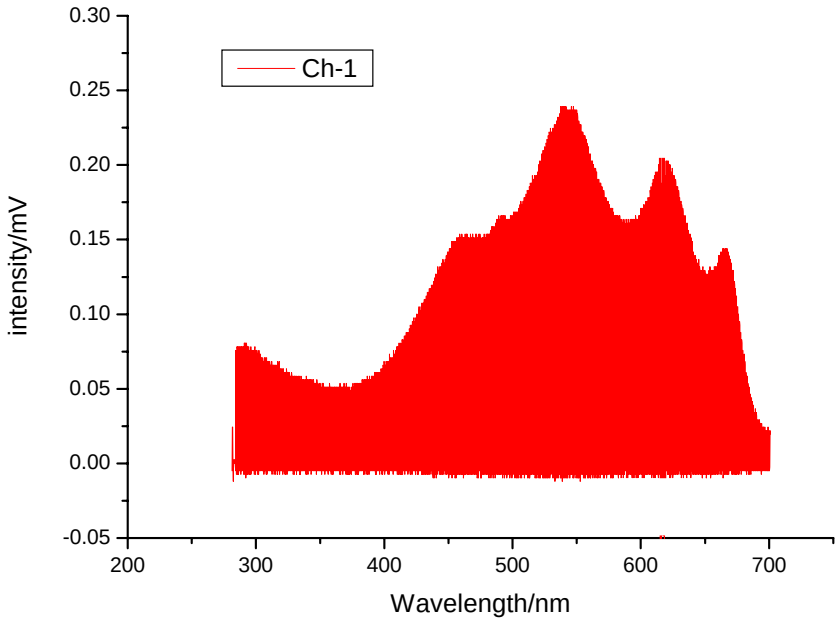

Figure 9: Typical spectrum of the probe light recorded by photodiode array detector.

References

(1) H. A. Haus, K. Tamura, L. E. Nelson and E. P. Ippen, J. Quant. Electr., 31, 591, **1995**.

(2) L. E. Nelson, D. J. Jones, K. Tamura, H. A. Haus and E. P. Ippen, Appl. Phys. B, 65, 277 **1997**.

(3) D. E. Spence, P. N. Kean, and W. Sibbett, Optics Letters 16 (1), 42-44, **1991**.

(4) Demtröder, W., Laser spectroscopy. Berlin, Springer, **2003**.

(5) Van Hecke, G. R. A guide to lasers in chemistry, Boston, Jones and Bartlett Publishers **1998**.

(6) Wilhelm, T., J. Piel, et al.. Optics Letters 22(19): 1494-1496, **1997**.

(7) Lochbrunner, S., P. Huppmann, et al. Optics Communications, 184(1-4): 321-328 **2000**.

(8) Riedle, E., M. Beutter, et al. Applied Physics B-Lasers And Optics, 71(3): 457-465, **2000.**

(9) Kovalenko, S. A., A. L. Dobryakov, et al.. Physical Review A 59(3): 2369-2384. **1999.**

(10) A. I. Belousov, S. A. Verzakov, Humboldt University, Berlin, Germany, **1999.**

(11) R. Bonneau, J. Wirz, A. D. Zuberbühler, Pure & Appl. Chem., , 69, 979, **1997.**

(12) Harald Gampp, Marcel Maeder, Charles J. Meyer, and Andreas D. Zuberbühler, Talanta, , 32, 257-264, **1985.**

(13) Y. R. Shen, The Principles of Nonlinear Optics, Wiley, New York, **1986**.

(14) D. T. Reid, W. Sibbett, J. M. Dudley et al., Applied Optics 37 (34), 8142-8144 (**1998**).

(15) Gavin D. Reid and Klaas Wynne, Ultrafast Laser Technology and Spectroscopy in Encyclopedia of Analytical Chemistry, R.A. Meyers (Ed.), 13644–13670, John Wiley & Sons Ltd, Chichester, **2000**

(16) M. Dantus, R. M. Bowman and A. H. Zewail, Nature 343, 737 (**1990**).

(17) L. Dhar, J. A. Rogers, and K. A. Nelson, Chemical Reviews 94 (1), 157-193 (**1994**).

2. Photochemistry of 3-diazo-2-oxindoline

2.1. Introduction

The chemistry of α-diazocarbonyl compounds is usually associated with the Wolff rearrangement[1,2], a versatile reaction that has found wide application in diverse areas of research and technology. Recent studies of α-diazocarbonyls have helped to clarify their chemistry and furthered understanding of the mechanisms underlying the complex reactivities of α-diazocarbonyl compounds.

2.1.1 Carbenes

α - Diazocarbonyl compounds of which the photochemistry is studied in this work, as well as many other diazo compounds are known to react through a carbene intermediate upon irradiation. Carbenes are important intermediates in a variety of chemical reactions and have therefore been extensively studied both experimentally and theoretically[3,4].

They are neutral, divalent derivatives of carbon. The majority of carbenes are short-lived. The nonbonding electrons of the carbene carbon atom can be spin paired (singlet state) or unpaired (triplet state). The two electronic states have different electronic configuration and each state exhibits different reactivity and is affected differently by the substituents.

In general, the singlet state undergoes concerted reactions with high efficiency, the triplet state on the other hand is a less reactive and selective reagent.

Since the carbene's reactivity is state specific, the magnitude of the singlet-triplet (S-T) splitting is of great importance and has received particular attention[5,6]. In reactions involving reactive intermediates, the most stable form usually plays a crucial role in controlling the reaction pathway. However, in reactions of carbenes, the reaction is not always initiated from the ground state. This is especially true in the reactions of triplet ground state carbenes with a small S-T gap.

In a singlet carbene, the paired electrons occupy an s orbital, leaving a p orbital vacant. Since two electrons are constrained to the same small molecular orbital, electron – electron Coulombic repulsion is severe.

The triplet configuration is stabilized by relief of the Coulombic and exchange repulsion. A small energy difference between the s and p orbitals leaves the electrons unpaired (triplet). If a large gap exists between the s and p orbitals the electrons will pair in the s orbital (singlet). The separation of the electrons into different molecular orbitals does not come without a cost. A small difference between the energies of S_0 and T_1 may easily be overturned by the effect of substituents or even solvents.

Singlet carbenes are stabilized by electron donation from substituents into the vacant p orbital. In terms of resonance, the contribution of an ylide structure is implied. Push–pull stabilization is also conceivable.

It has been shown that singlet states are stabilized relative to the triplet states in polar solvents. This is mainly due to the dipole interaction of solvent with the singlet carbene. There is a good correlation between ΔG_{ST} and the solvent polarity parameter $E_T(30)$ indicating that specific carbene – solvent complexes do not play a significant role in determining carbene stability for the solvent used. In general, rates of reaction from the singlet state are larger than of triplet. The rate of singlet to triplet intersystem crossing and the reverse rate are related to ΔE_{ST} according to the Arrhenius equation.

When ΔE_{ST} is less than ~ 3 kcal/mol, singlet - triplet equilibration is usually assumed. Thus, the multiplicity that is involved in the reaction can be summarized as follows[7].

1. Carbenes with a singlet ground state far below the triplet react in the singlet state even if generated by triplet sensitized photolysis.
2. Carbenes with a triplet ground state well separated from the singlet ($\Delta E_{ST} > 5$ kcal/mol) react in a multiplicity determined by the method of generation.
3. Carbenes with a triplet ground state and a small energy separation ($\Delta E_{ST} < 3$ kcal/mol) react in the singlet state regardless of the method of generation.

2.1.2 Photochemistry of α - diazo ketones

Many photochemical reaction pathways are conceivable for α - diazocarbonyl compounds[8,9]. Scheme 1 summarizes some of them. Photolysis of α - diazo ketones produces an excited singlet state, which can suffer nitrogen loss and singlet carbene formation, isomerization of the diazo group to a diazirine or intersystem crossing to the triplet diazo compound[10]**.** The triplet carbene can be in rapid equilibrium with the singlet carbene. Alternatively, the triplet excited state of α - diazo ketone can extrude a nitrogen to form the triplet carbene. Oxygen is a known selective trap of triplet carbenes. The products of this reaction are carbonyl oxides. Carbonyl oxides are extremely photolabile even under matrix conditions and irradiation with red light (600nm) rapidly produces dioxiranes[7]. Dioxiranes can be converted by 400 nm light into esters or lactones. In the dark, extrusion of oxygen producing ketones becomes their main reaction pathway.

The yield of α - carbonyldiazirines depends on the wavelength of irradiation of the parent diazocompound and they might undergo thermal or photochemical reverse isomerization[11] into the parent diazo compound or loose nitrogen to give an α – carbonylcarbene. Interconversion of some isomeric carbonyl carbenes via oxirenes have been detected by means of isotopic labeling or by scavenging of isomeric carbonyl carbenes.[2] The interconversion is affected by carbene stabililities, conformational effects and (or) migratory aptitudes.

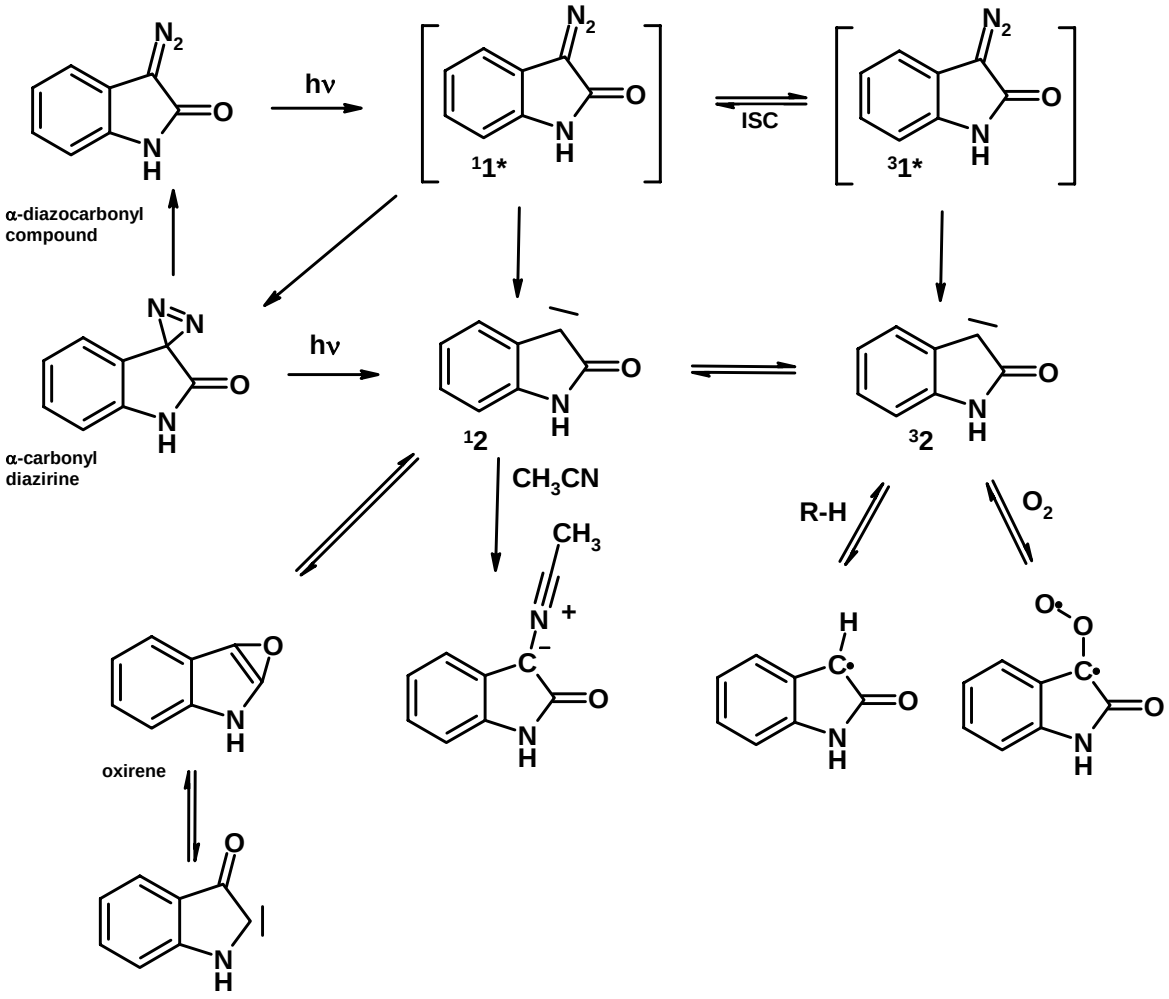

Scheme 1: Possible photochemical reaction pathways of 3-diazo-2-indolinone.

Carbenes react readily with nucleophiles like piperidine forming ylides[12,13]. Such a trapping reaction is often used to identify carbene intermediates since piperidine ylides have characteristic absorption band around 400-450 nm where other transients usually do not absorb.

Scheme 2 shows possible reaction pathways of singlet α-carbonylcarbene in water or a water containing solution[14]. A key reaction of singlet carbonyl carbenes (YC-CO-X) is the Wolff rearrangement, leading to the production of ketene.

The Wolff reaction is a key step in many experimental methods, such as synthesis of small strained ring systems by ring contraction, preparation of α-ketoacid derivatives, photoaffinity labeling, DNA photocleaving, and nanomachining. The most important industrial application of the Wolff rearrangement is found in photolithography, a process used in the production of electronic microchips and integrated circuit boards[11].

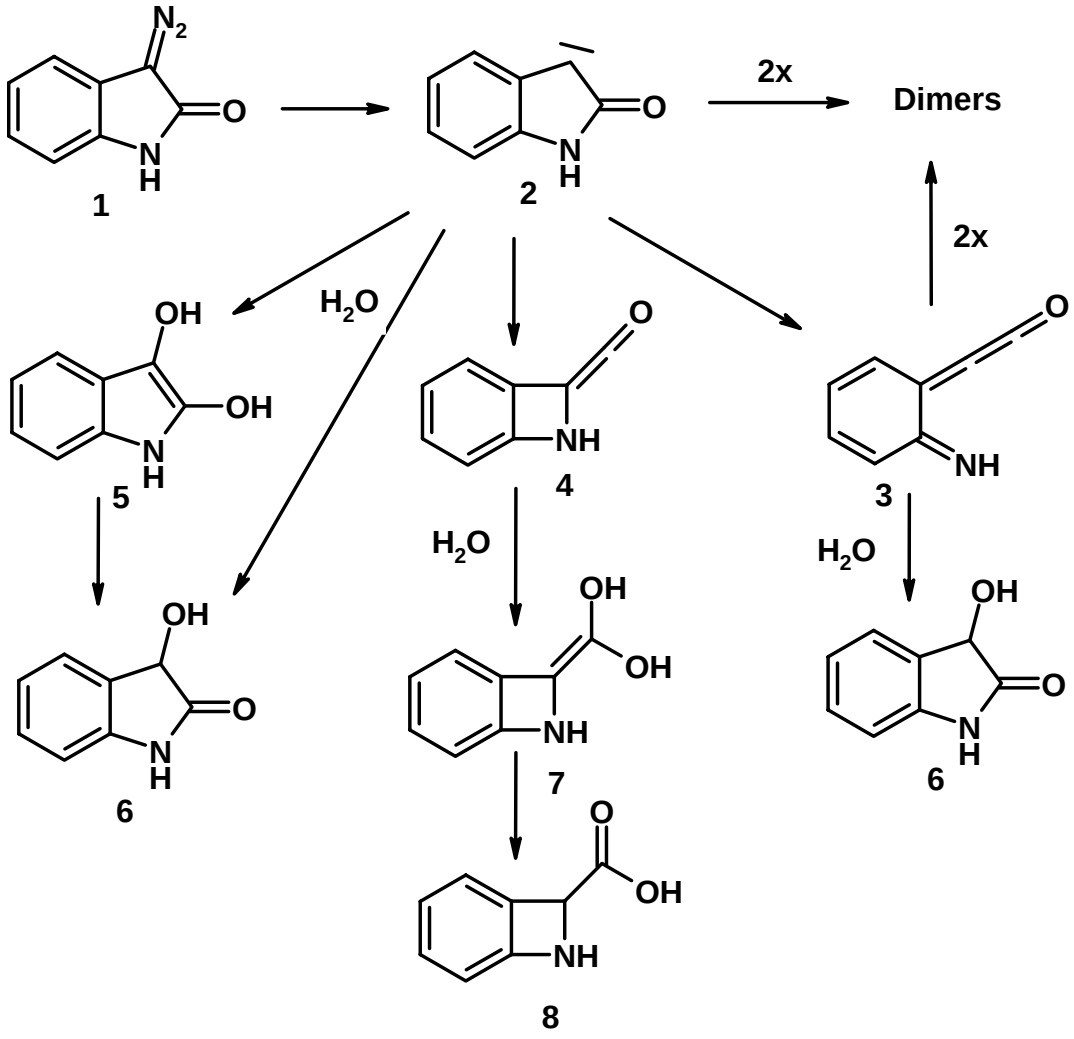

Scheme 2: Reaction pathways of the α-carbonyl carbene in aqueous solutions.

The α-carbonylcarbene formed by dediazotization of 1-diazo-2-indanone derivatives has more options for further intramolecular reaction. (CO)-X ring cleavage to the quinonoid

cumulenone, Wolff-rearrangement to the cyclic ketene. Another possibility is reaction with water via O-H insertion.

The Wolff rearrangement produces a ketene, which, in aqueous solution, becomes hydrated to a carboxylic acid. The rearrangement can occur in concerted manner directly from excited singlet state of the diazo carbonyl compound or from carbene intermediate.

Hydrolysis of the cumulenone in aqueous solutions is initiated by rate-determining protonation. The final product is expected to be the same as in the case of OH insertion.

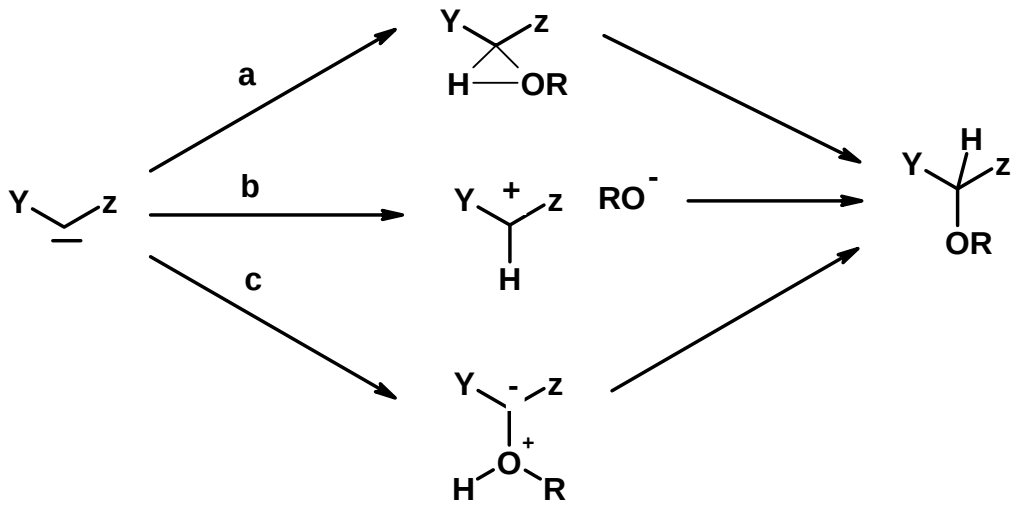

3 mechanisms are generally discussed for insertion of carbene into a OH bond[8,15]:

a, a concerted O-H insertion,

b, protonation of the carbene to give a carbocation[16] (or protonation of the diazo compound to give a diazonium ion which subsequently loses nitrogen)

c, nucleophilic attack on the electrophilic carbene to give an ylide followed by hydrogen transfer.

In the case of α-carbonyl carbenes, the proposed oxygen ylide could also undergo proton translocation from the hydroxylic oxygen to the carbonyl oxygen

to give an enol, which would subseqently ketonize, forming more stable α-alkoxycarbonyl compound.

Although the concerted pathway (a) cannot be completely excluded, there is no direct experimental evidence to support it, and it is likely that most, if not all, O-H insertions reactions of carbenes proceed by one of the stepwise processes (b) or (c).

Irradiation of 1-diazo-2-indanone derivatives in aprotic solvents usually yields a mixture of dimers. Their structure and ratio may depend on the reaction mechanism. The quinonoid cumulenone, for example, has more possibilities for dimerisation than a carbene. Insertion of a carbene into diazo group of starting material is common in aprotic solvents, too.

2.1.3 Photochemistry of 1-Diazo-2-indanone and similar derivatives.

In 1964 Moriconi and Murray studied the photochemistry of 1-methyl-3-diazooxoindole[17]. They reported 3-methoxy-1-ethyloxindol as a product of photolysis in very dilute ethanol solution under nitrogen.

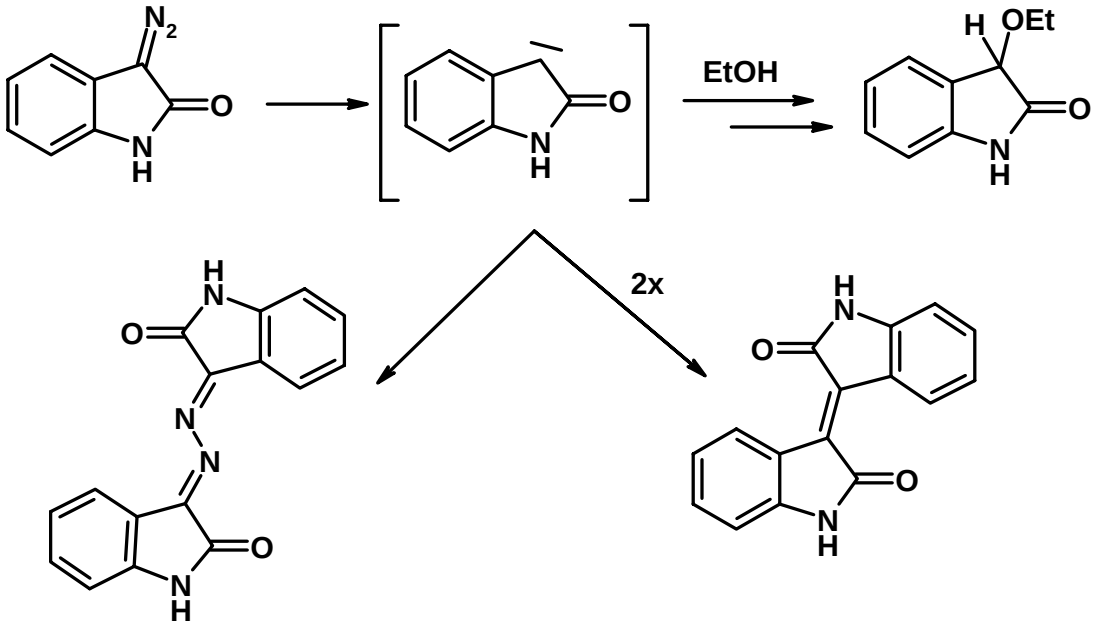

The α-ketocarbene singlet was found to be an intermediate on the base of trapping reactions with nucleophiles. The absence of any ring contraction product was noted.

Voigt and Meier studied the 3-diazooxoindole and its methyl derivate some years later[18,19]. They observed major (95%) methyloxindol product and dimerisation products isoindigo and azin to be formed. The valence isomerism of diazo and diazirine group was found as well.

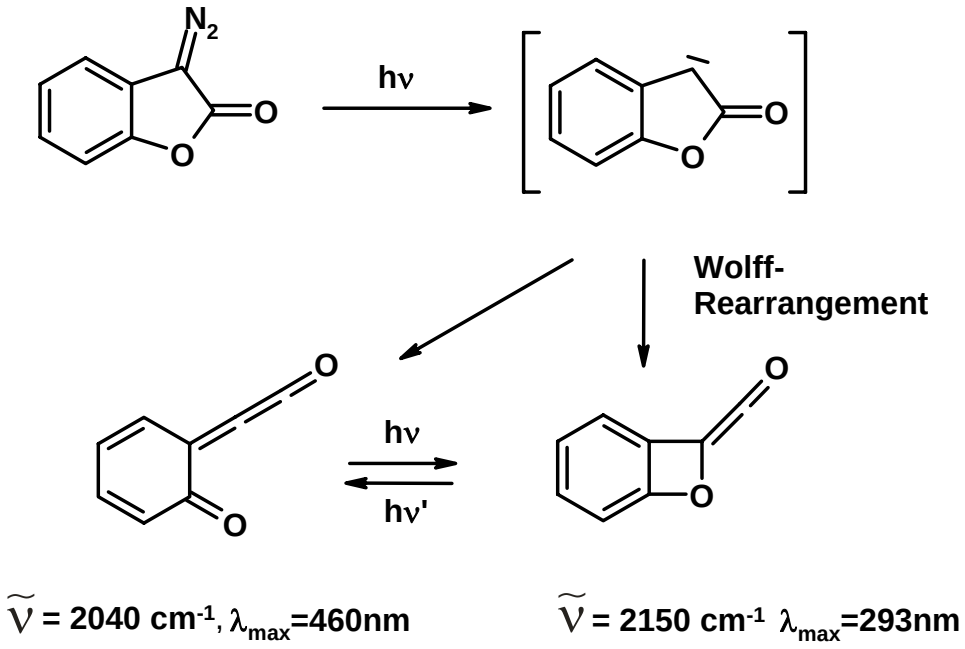

Low temperature matrix experiments[20] done by Chapman and co-workers showed two products after irradiation of 3-diazobenzofuran-2-one. The photoproducts readily interconvert photochemically with long wavelength (>350nm) light favoring the ketene and short wavelength light (254nm) favoring the quinonoid cumulene. A carbene intermediate was not observed.

Soon after, Voigt and Meier reported[21] formation of 2-(2-hydroxyphenyl)-2-methoxyacetic acid methyl ester upon irradiation of 3-diazobenzofuran-2-one in methanol solution. These authors considered several reaction paths and concluded that the reaction proceeds either by direct O-H insertion of the carbene into methanol or via the cyclic ketene.

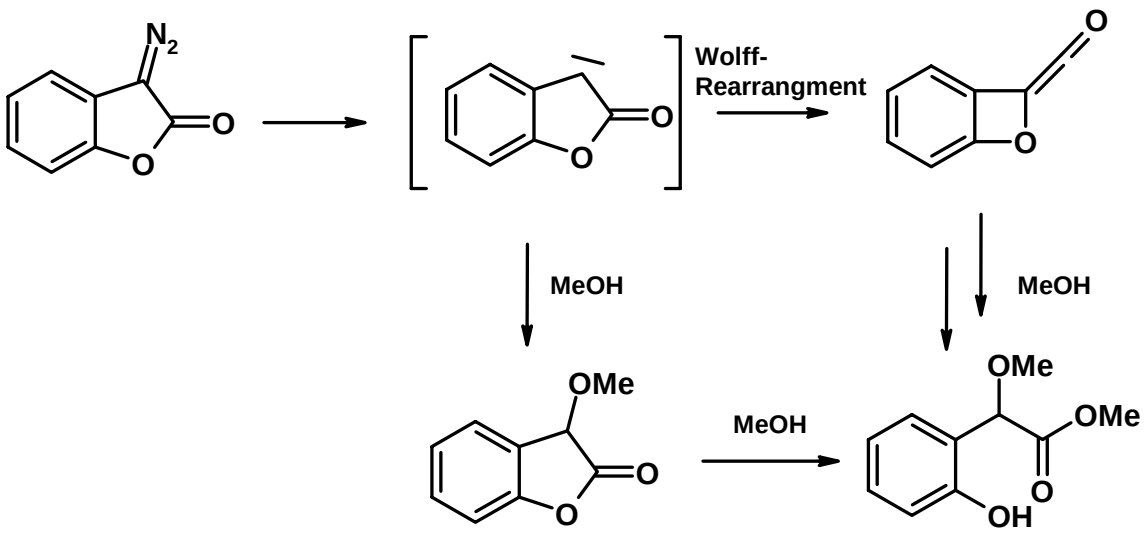
N2
O
O
Wolff-
Rearrangment
O
O
MeOH
MeOH
OMe
MeOH
OMe
O
O
O
OH

References

(1) Wolff, L. Justus Liebigs Ann. Chem., 325, 129-195, **1902.**

(2) Kirmse, W.. European Journal Of Organic Chemistry (14): 2193-2256, **2002.**

(3) Toscano, J. P. Advances in Carbene Chemistry; Brinker, U. H., Ed.; JAI Press: Greenwich, CT, Vol. 2, p 215, **1998.**

(4) Kirmse, W. In Brinker, U. H., ed., Advances in Carbene Chemistry; JAI Press: Greenwich, Conn.; vol. 1, pp. 1-58, **1994.**

(5) Scott, A. P., M. S. Platz, et al.. Journal Of The American Chemical Society 123(25): 6069-6076, **2001.**

(6) Wang, Yuhong; Hadad, Ch., M.; Toscano, J. P., Journal of the American Chemical Society, 124(8), 1761-1767, **2002.**

(7) Tomioka, H., Triplet carbenes. in Reactive Intermediate Chemistry, 375-461, **2004.**

(8) Miller, D., Moody J., Tetrahedron, 51(40), **1995.**

(9) Tomioka, H., Nitrogen, Oxygen and Sulfur Ylide Chemistry, 213-218, **2002.**

(10) Toscano, John P.; Platz, Matthew S.; Nikolaev, Valerij; Popic, Vladimir., Journal of the American Chemical Society, 116(18), 8146-51, **1994.**

(11) Bogdanova, A.; Popik, V., Journal of the American Chemical Society, 125(46), **2003.**

(12) Olson, D. R.; Platz, M. S., Journal of Physical Organic Chemistry, 9(11), 759-769. **1996.**

(13) Platz, M. S.; Olson, D. R., Journal of Physical Organic Chemistry, 9(10), 689-694, **1996.**

(14) Gaplovsky M., Boudebous H., Wirz J.,Versatile Carbenes from 1-Diazo-indan-2–one Derivatives, 7th International Conference on Reaction Mechanisms, Dublin July, **2004**

(15) Chiang, Y., E. A. Jefferson, et al. Journal Of Physical Organic Chemistry 11(8-9): 610-613, **1998.**

(16) Schepp, N. P. and J. Wirz. "Effect Of Alpha-Carbomethoxy Group On The Reactivity Of Benzyl Cations In Solution." Journal of The American Chemical Society 116(26): 11749-11753, **1994.**

(17) Moriconi, E., J.; Murray, J. J., Pyrolysis and photolysis of 1-methyl-3-diazooxindole. Base decomposition of isatin 2-tosylhydrazone. Journal of Organic Chemistry, 29(12), 3577-84, **1964.**

(18) Voigt E., Meier H., Diazirines as photochromic valence isomers of α-diazocarbonyl compounds. Angewandte Chemie, 87(3), 109-10, **1975.**

(19) Voigt E., Meier H., Valence isomerism of diazo compounds and diazirines. Chemische Berichte, 108(10), 3326-35, **1975.**

(20) Chapman, O. L.; Chang, C. C.; Kolc, J.; Rosenquist, N. R.; Tomioka, H. Photochemical method for the introduction of strained multiple bonds. Benzyne C .tbd. C stretch., Journal of the American Chemical Society, 97(22), 6586-8, **1975.**

(21) Voigt E., Meier H., Photochemistry of heteroanalogous 3-diazo-2-oxoindanes. Chemische Berichte, 110(6), 2242-8, **1977.**

2.2. Pump - probe experiments

Ultra fast absorption pump - probe spectroscopy was used to investigate processes directly following the excitation of the compounds studied, where the pico- and sub-picoseconds time resolutions are needed.

The measurements were done in various solvents, namely water, acetonitrile, dichlomethane, methanol and solvent mixtures (water/acetonitrile). Solutions of studied diazo compounds in 10^{-2} – 5 x 10^{-4} concentrations were excited at 270 nm. The laser beam had a pulse length (FWHM) 150-200 fs. Transient spectra were collected within the range from 300 to 600 nm.

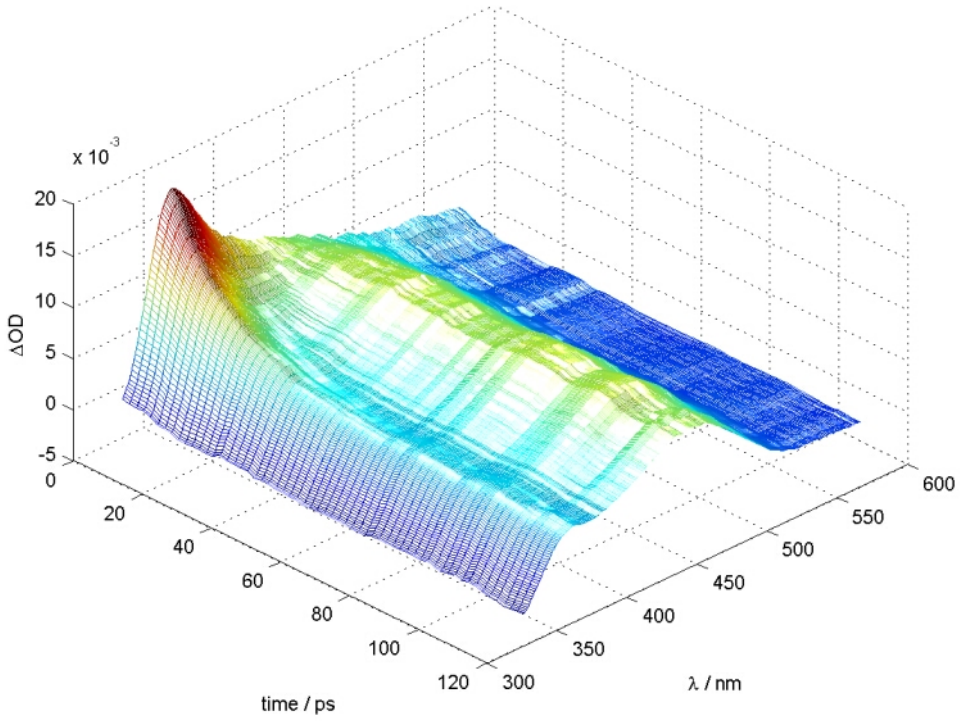

Figure 1: 3D visualisation of transient's absorption within the first 120ps after the excitation of 3-diazo-2-indolinone in neat acetonitrile

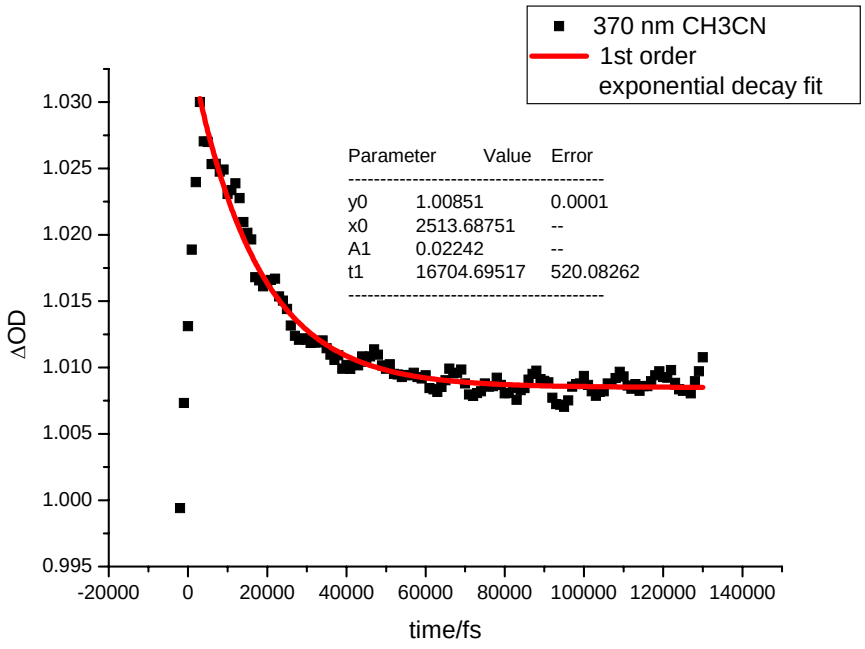

Figure 2: Kinetic trace and the best fit of 3-diazo-2-indolinone transient at 370nm in neat acetonitrile.

First measurements over the available time delay of 1.8 ns showed a relatively weak and stable absorption band in dry acetonitrile at λ_{max} = 450 nm. A Closer investigation of the first 150 ps revealed a second band with maximum around 370 nm, which decayed with a lifetime of 17 ps.

A weak growth of absorption was observable at 450 nm. This was completed within 30 ps. It would be very difficult to fit reliably the kinetics of this growth due to the poor signal-noise ratio even after component analysis. Repeated experiments in water have not revealed any change in 300-600 nm absorption on the lower nanosecond time scale except long-lived structureless absorbance by solvated electrons. However, when we decreased the time step of the experiment to 100 fs we could observe stronger 370 nm absorbance immediately after excitation, decaying within 3 ps. Correction of time chirp caused by group velocities dispersion was necessary in this case.

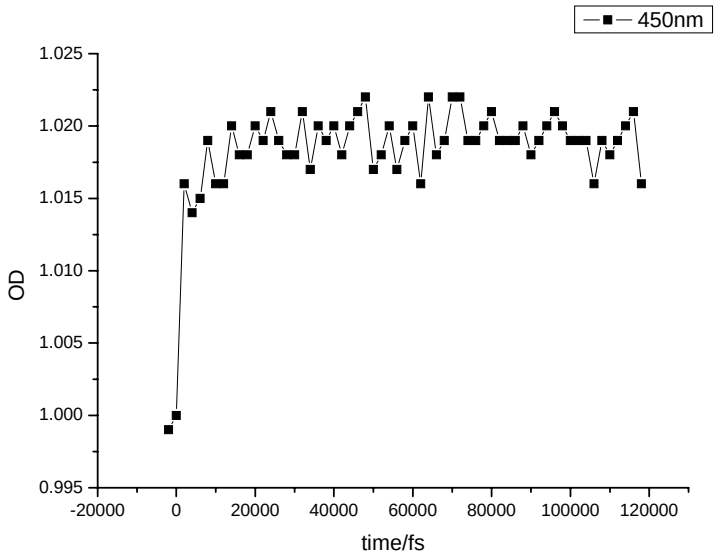

Figure 3: Formation of the transient at 450nm in acetonitrile.

In order to get more information on the photochemistry of diazoindolinone in water, a series of acetonitrile – water solutions of the compound at different mixing ratios were examined by pump-probe spectroscopy.

% of water in acetonitrile	Conc. of H_2O [mol/l]	lifetime of transient at 370 nm	relativeAbsorbance at 450 nm 100 ps after excitation
0	0	16.7	0.034
15	8.25	11.1	0.0245
20	11	9.84	0.02219
25	13.75	8.32	0.02245
30	16.5	7.02	0.0152
50	27.5	3.86	0.01482

Table 1: Lifetimes of singlet carbene followed at 370 nm absorption decay and relative absorbance of cumulene at various water concentrations in acetonitrile.

Two trends were clearly recognizable. First, the lifetime of 370 nm transient shortens with increasing concentration of water. On the other hand, the water concentration does not affect intensity of the 370 nm transient.

The second trend is a decreasing amount of the 450 nm transient with increasing H_2O concentration. It was not observable at all at 98% water concentration.

The photolysis of 3-diazo-2-oxoindoline in methanol solutions produces absorbance at 360 nm that is a main feature of the spectra shortly after the excitation and decays with a lifetime of 7.2 ps. At 450 nm a very weak transient is formed within 30 ps and is stable over the maximum time delay of 1.8 ns.

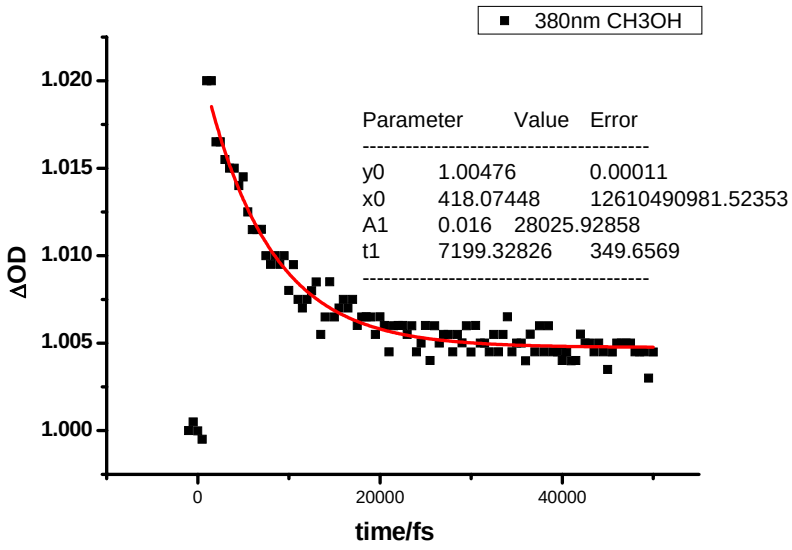

Figure 4: Kinetic trace and best fit of transient at 370nm in neat methanol.

Dichloromethane has the lowest polarity and the dielectric constant of all studied solvents. There was a weak band at 460 nm formed immediately after the excitation. Surprisingly, it kept on growing 1.7 ns after excitation. 370 nm band was also observed although its intensity was weaker than in other solvents.

2.2.1 Discussion

The structures, which can exist straight after the excitation at 270 nm are either excited state of diazoindolisine, or more likely, the primary photoproduct of the reaction, a carbene in either singlet or triplet state[1]. Hess and co-workers studied recently ultra fast

carbonylcarbene formation and equilibration by femtosecond pump - probe spectroscopy[2]. Their results indicate that singlet and triplet carbenes are formed on the time scale of a several hundred femtoseconds with a large amount of excess the internal energy. The spin equilibration occurs within the photodissociation and thermalization of the hot photoproduct. They assigned observed absorption bands to particular species on the base of electronic spectra of both singlet and triplet carbene obtained by low temperature matrix spectroscopy[3].

Unfortunately, we do not have information from matrix spectroscopy. We have however a reasonable estimate of the singlet-triplet gap from high-level calculations. $\Delta E_{ST} \sim 5$ kJ/mol is obtained in the gas phase with a triplet ground state on G3MP2B3 level. This gap is likely to be even smaller or inverse in polar solvents[4].

Very little information is available about the photodissociation dynamics of diazo compounds. It is proposed[5] that N_2 loss occurs promptly, perhaps on the time scale of a single C-N stretching period. The excited state absorption should be distinct from the carbene spectra because of the very different electronic structure of carbenes and their diazo precursors.

The 370 nm transient seems to be quenched rapidly by the solvent when it is water or methanol, most likely by O-H insertion. The only transient known to give this reaction on a time scale of picoseconds is a singlet carbene. It is known that singlet carbenes react in alcohols via O-H insertion to form far UV-absorbing ethers[6]. Indeed, no rising signals were observed above 300 nm. The expected UV band could not be directly observed due to weak probe intensity in UV spectral domain.

We assume that the observed processes may be described by scheme 1. Excitation of 3-diazo-2-oxoindoline produces an excited state, which suffers nitrogen loss forming a cumulene in neat acetonitrile. The yield of cumulene (A_{cum}) is reduced to (A'_{cum}) upon excitation of 3-Diazo-2-oxoindoline in the presence of a competitive carbene quencher which is water in our case. The same holds for singlet carbene lifetime τ, which becomes shorter with increasing concentration of water.

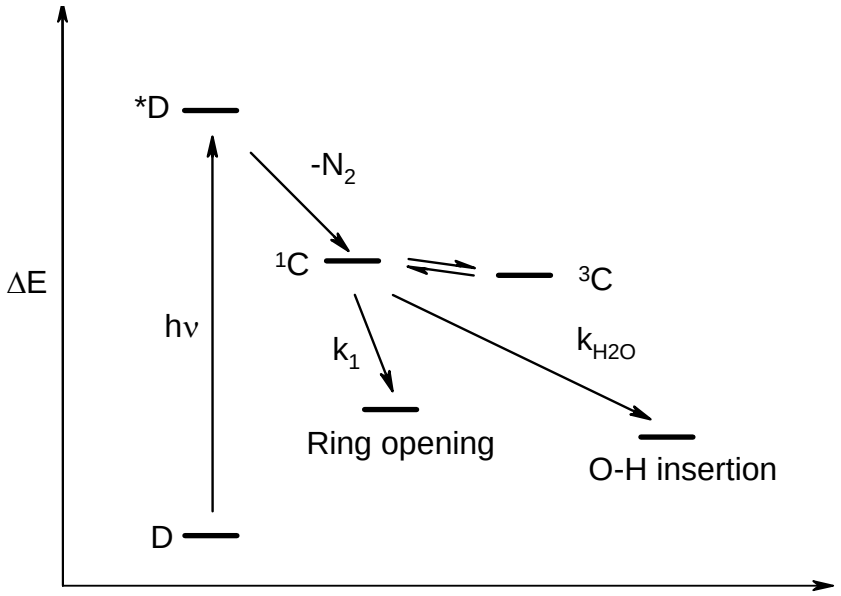

Scheme 1: Deactivation of 3-Diazo-2-oxoindoline singlet excited state

In order to get information on the carbene-water reaction rate we plotted τ^0/τ versus water concentration (Figure 1) according to Stern-Volmer equation:

$$\tau^0/\tau = 1 + k_q\tau^0[H_2O]$$

A Stern–Volmer treatment of the quenching data is linear with slope $k_q\tau^0$ where τ^0 is 16.7 ps and k_q is the absolute rate constant of spin equilibrated carbene with quencher when $k_q = k^s_qK$. The value of k_q calculated from our data was 7 x 10^9 $mol^{-1}s^{-1}$.

Similarly, we can express quantum yield of cumulene ϕ_{cum} on the base of the scheme 1 using equation:

$$\phi_{cum} = \phi_{^1C} * (k_1/(k_1 + k_q * [H_2O])),$$

where ϕ_{1c} is quantum yield of singlet carbene, k_1 ring opening rate and k_q as before. The quantum yield of cumulene can be approximately substituted by absorbance at 450 nm relative to the initial carbene absorbance (370nm) in the particular measurement.

$$1/\phi_{cum} \approx 1/A_{cum} = Const * ((1 + k_q * [H_2O])/k_1)$$

We fitted the plot of $1/\phi_{cum}$ versus water concentration in Mol/l. The slope of the straight line fitted to the data point by least square method is equal to the ratio between k_q and k_1

multiplied by the constant. The constant equals to the value $1/\phi_{cum}$ at zero water concentration. So we can write:

$$k_q / k_1 = \text{Slope} / \text{Const}$$

Hence, $k_q = 3.4 \times 10^9\ mol^{-1}s^{-1}$, assuming that $k_1 = 16.7$ ps. The difference around 50% in k_q calculated by two methods can be probably assigned to the rough approximations of the second calculation or alternatively part of the cumulene may be formed directly from excited singlet state of the studied diazo carbonyl compound. Nevertheless, these Stern – Volmer plots clearly indicate that the carbene is a precursor of the cumulene and in the presence of water undergoes a competitive reaction, which proportionally decreases cumulene quantum yield.

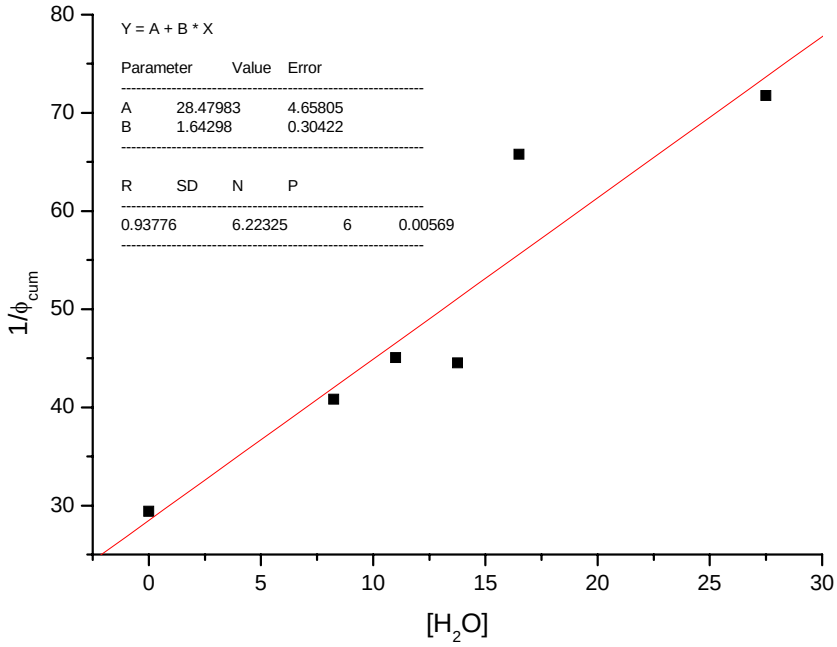

Figure 5: A plot of $1/\phi_{cum}$ vs $[H_2O]$, obtained by pump-probe spectroscopy in acetonitrile containing water 100 ps after the excitation.

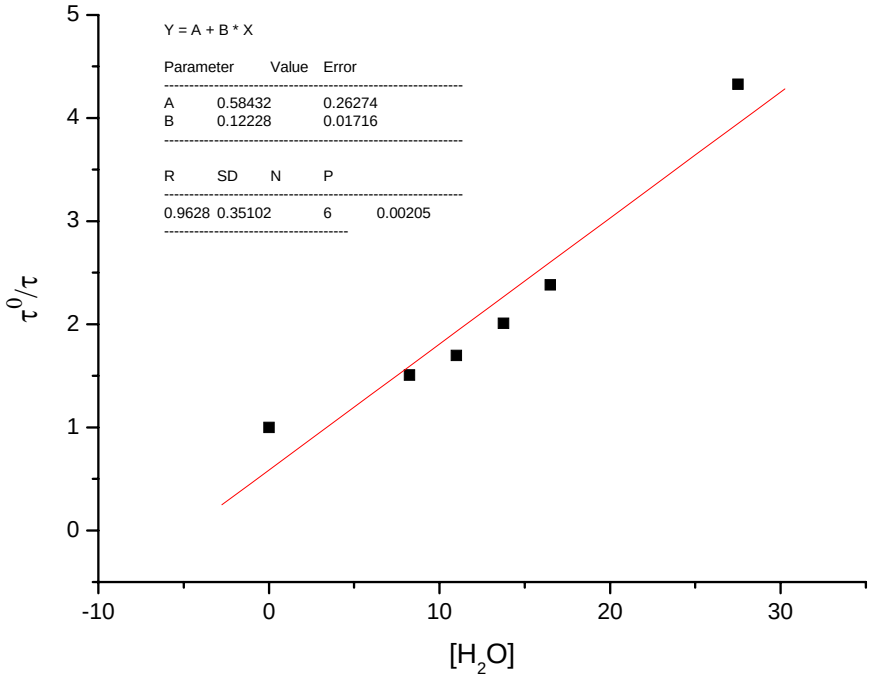

Figure 6: Stern–Volmer treatment of the quenching of the carbene lifetime with water in acetonitrile

The 450 nm bands in acetonitrile, dichloromethane and methanol agree in shape and position with those measured by Laser Flash Photolysis at longer time scales.

As can be seen on Figure 3 the absorbance at 450nm is formed to a substantial extent within the resolution of our instrument but keeps on growing next 30 picoseconds in pure acetonitrile. Most of the cumulene formation is probably hidden or covered by some other process that may take place, for example excited state decay or intersystem crossing of excited diazo carbonyl or carbonyl carbene. Thermal relaxation of singlet carbene may also contribute to the absorbance evolution at 450nm. Moreover, equilibration of transitions moments on the base of rotational diffusion makes the kinetics even more complicated (see the setup description). The reliable global analysis can not be done on the basis of these results without additional information on transient spectra.

References

(1) Toscano, J. P., Platz, M. S.; Nikolaev, V., Journal of the American Chemical Society, 117(16), 4712-13, **1995**.

(2) Hess, G. C.; Kohler, Bern; Likhotvorik, I.; Peon, J.; Platz, M. S., Journal of the American Chemical Society, 122(33), 8087-8088, **2000**.

(3) Zhu, Z.; Bally, T.; Stracener, L. L.; McMahon, R. J., Journal of the American Chemical Society, 121(12), 2863-2874, **1999**.

(4) Geise, C. M.; Wang, Y.; Mykhaylova, O.; Frink, B. T.; Toscano, J. P.; Hadad, Ch. M., Journal of Organic Chemistry, 67(9), 3079-3088, **2002**.

(5) Yamamoto, N.; Bernardi, F.; Bottoni, A.; Olivucci, M.; Robb, M. A.; Wilsey, S. J. Am. Chem. Soc., 116, 2064, **1994**.

(6) Elsaesser, T.; Kaiser, W. Annu. ReV. Phys. Chem., 42, 83, **1991**.

2.3. Nanosecond laser flash photolysis.

Flash photolytic fast reaction techniques have proven to be especially useful in studying unstable short-lived species, therefore we have employed such techniques to investigate the mechanism of 3-diazo-2-indolinone photoreaction in nano- to millisecond time domains.

Flash photolysis in pure acetonitrile solutions produced a transient absorbance with λ_{max} = 450 nm immediately after laser pulse. This transient then decayed over a period of ca 300 μs following a dual exponential kinetics, while another transient absorbance with λ_{max} = 310 nm grew in and then also decayed. The first decay rate at 450 nm $k_1 = 2 \times 10^5$ s^{-1} was the same as the rate of the rise at 310 nm indicating that the 310 nm transient is formed from that at 450 nm. This rate was not influenced by the laser intensity or concentration of the solution. In addition, the decay rate of 310 nm absorbance equals second component of 450 nm absorbance decay. The second rate constant seemed to be concentration dependent indicating pseudo-first order behaviour. In order to uncover the spectral shape of the transient absorbance, several spectra with different delay times after the laser flash were taken.

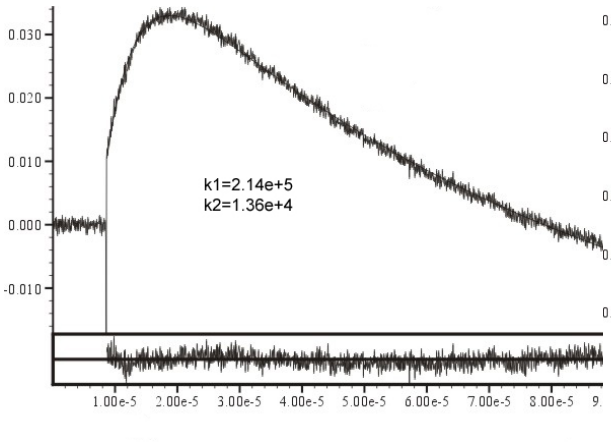

Figure 1: 305 nm transient kinetic trace in acetonitrile

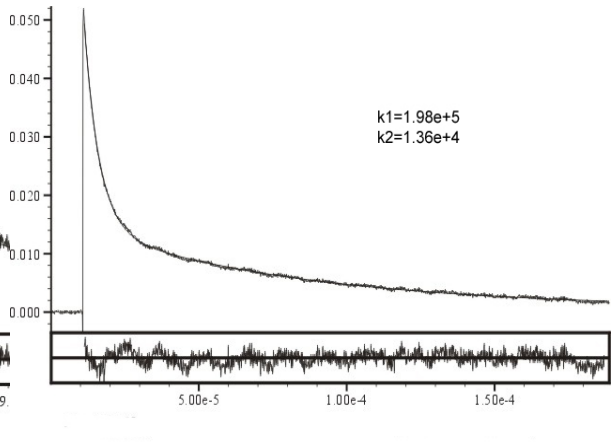

Figure 2: 450 nm transient kinetic trace in acetonitrile

Their comparison with the pump probe 450 nm transient spectra confirms that it is the same species. A very similar picture was observed in dichloromethane, chloroform and pentane. The two first- order decay rates of the 450 nm transient are practically the same as in the acetonitrile. In isooctane, however the second lifetime is two orders of magnitude longer then in other solvents.

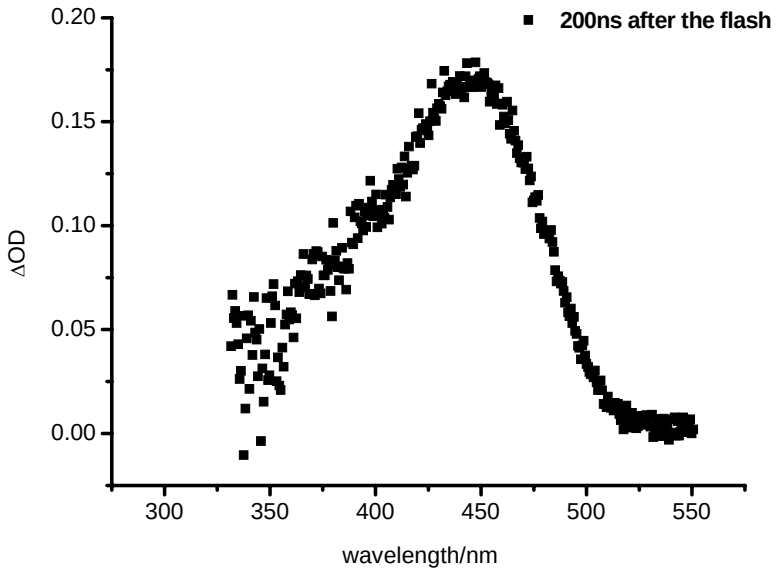

Figure 3: Transient absorbance spectra in acetonitrile 200 ns after the flash.

In the wet acetonitrile solutions, the 450 nm transient lifetime depends on the concentration of water. Already at a concentration of 2.5 % water is the kinetic trace clearly first order. This indicates that the 450 nm transient is intercepted by water molecule. Besides the lifetime, also the intensity of the transient decreases with increasing water concentration and disappears totally at 40 % of water. This observation is in agreement with pump - probe spectroscopy results where the 450 absorbance also decreases with increasing water/acetonitrile ratio.

Some of the solutions were analysed by GS-MS and TLC, only one product was observed. Its retention time (with or without coinjection), R_F value and mass spectra corresponded to the 3-hydroxy-2-indolinone standard.

In weakly acidic aqueous solution the laser photolysis produced only one weak transient with A_{max} = 270 nm, which then decayed following first order kinetics. The rate depended strongly on the acid concentration. In the neutral and very weak basic solutions ([NaOH] = 10^{-4}) was the kinetics more complex since the transient decaying at 275 nm produced another one at around 310 nm which subsequently decayed.

Measurements in basic solutions were complicated by instability of the 3-diazo-2-oxindolinone. The amide linkage is reported to be labile to ring cleavage with dilute base. This complications and further increase of the whole process complexity discouraged us from examining the photochemistry in more basic solutions. In order to reveal the character of 270 nm transient, the rates of its decay were measured as a function of the solution pH. Aqueous perchloric acid, biphosphate, acetate and borate ion buffers were used to keep the required pH. For buffer solutions, a range of concentration was employed at one pH point to estimate possible general acid catalysis rate and replicate measurements were made at each concentration. The ionic strength was maintained constant at 0.1 M by adding the required amount of sodium perchlorate.

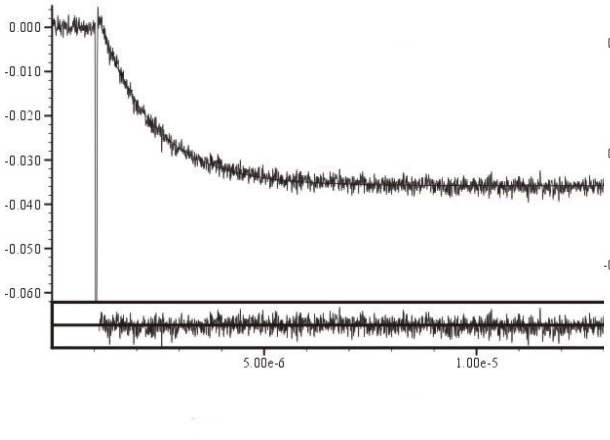

Figure 4: 270 nm transient kinetic trace in water pH 4

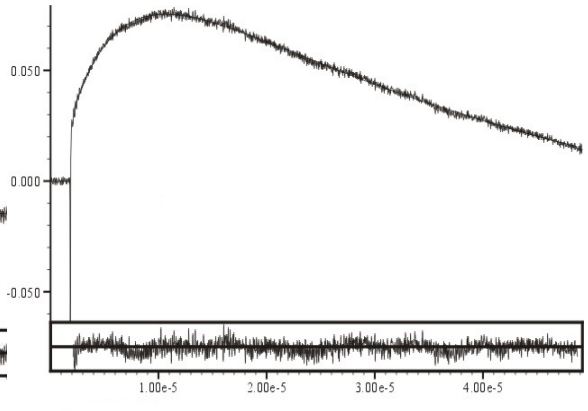

Figure 5: 285 nm transient kinetic trace in water pH 9

To get more information on the mechanism of the studied reaction, kinetic isotope effect was measured in deuterium oxide solution of perchloric acid over a concentration range 0.0002-0.0025 M. The ionic strength of these solutions was maintained at 0.1 M by adding sodium perchlorate.

Linear regression of these data produced hydronium ions catalytic coefficient $k_{H+} = 2.19\ 10^{10}\ M^{-1}s^{-1}$ and isotope effect $k_{H+}/k_{D+} = 1.14$

Some of the measurements were done in degassed solution to test possible oxygen effect on the reaction. We did not observe any change in comparison with aerated solutions.

2.3.1 Discussion

Pump-probe measurements in acetonitrile show formation of transient absorbance, A_{max} = 450 nm, with a rate constant of 7 x 10^{10} s^{-1} after femtosecond excitation of 3-diazo-2-oxoindoline. The 450 nm band agrees in shape and position with that reported for similar cumulenone[1] by Chapman et al., which helps to identify the present transient species. The same transient, Amax = 450 nm, was observed by nanosecond LFP in various solvents. We did not analyse these photolysed solutions of 3-diazo-2-oxoindoline in dry aprotic solvents. However, Moriconi and Murray as well a Voigt and Maier found the azine and isoindigo to be the main products in organic solvents[2,3]. Thus, the two exponential process observed at 450 and 310nm probably corresponds to reaction of cumulene with 3-diazo-2-oxindoline.

Our product study indicates that cumulenone **3**, once formed in wet acetonitrile solutions undergoes hydration to 3-hydroxy-2-indolinone. The Stern-Volmer plot (Figure 6) of the 450 nm transient quenching with water gives a $k_q = 1.88 \times 10^5\ M^{-1}\ s^{-1}$

Singlet carbenes can react with substrates by a number of plausible mechanistic pathways because of their zwitterionic nature. Alcohols also have the ability to react either as a Lewis acid or as a base. The amphiphilic nature of both, alcohols and carbenes is reflected in two possible reaction mechanisms that are commonly considered for the insertion of a-carbonylcarbenes into O—H bonds[4] (a) formation of an ylide through electrophilic attack of the carbene on an unshared electron pair of hydroxylic oxygen, followed by a 1,2-proton shift to give the final product, or (b) initial protonation of the

carbene to give a carbocation, which is then rapidly trapped by solvent. However, as Figure 7 illustrates, the proposed oxygen ylide could also undergo proton translocation from hydroxylic oxygen to carbonyl oxygen thus yielding an enol, which could then ketonize and form α- alkoxycarbonyl compound.

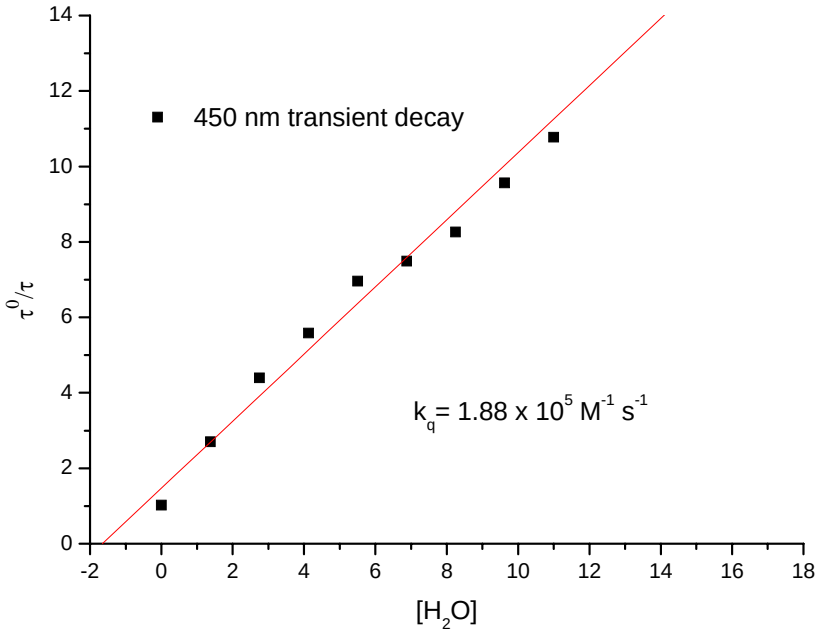

Figure 6: Stern–Volmer treatment of the quenching of the lifetime of 450 nm transient with water in acetonitrile

A number of studies on keto - enol tautomerization were published within last the years[5,6]. Most of them are based on the laser flash photolysis mesurements. For instance, Kresge and co-workers studied very similar structures as we do here, mandelamid and methylmandelate[7,8]. The pH profiles for ketonization of those compounds are in good agreement with the behavior expected for such a reactions (Figure 8).

The ketonization of enols is known to occur by rate determining protonation of the β-carbon atom of either the enol or the enolate ion, according to Figure 7. The rate profiles provide good evidence for this mechanism. They contain acid-catalyzed portions at low pH, as expected for carbon protonation of the nonionized enol by the hydronium ion.

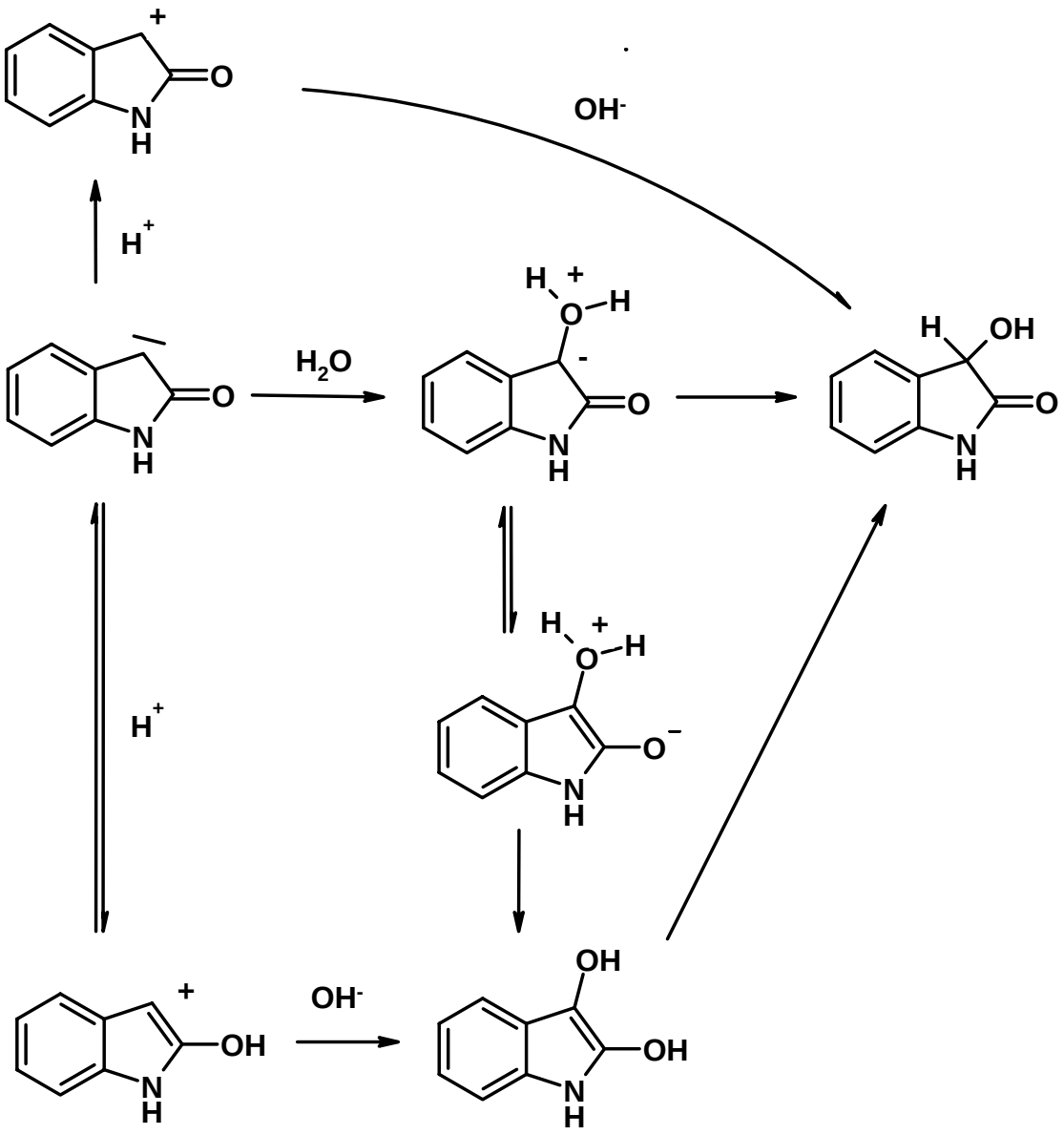

Figure 7: Possible reaction mechanisms that are commonly considered for the insertion of α-carbonylcarbenes into O—H bonds

This is then followed by a short 'uncatalyzed' region around $[H^+] \approx 10^{-4}$ M, which represents either protonation of enol by a water molecule or ionization of the enol to the much more reactive enolate ion followed by carbon protonation of enolate by hydronium ion. In the latter case, the fraction of enolate anion is inversely proportional to $[H^+]$, thus

giving the overall process the appearance of an "uncatalyzed" reaction. This portion of the rate profile is followed by a region of apparent hydroxide ion catalysis, in which enolate is carbon protonated by a water molecule. The fraction of ionized substrate is still inversely proportional to $[H^+]$, and so is the rate. Finally, when the position of the enol–enolate pre-equilibrium shifts over to enolate ion, this apparent hydroxide ion catalysis becomes saturated and another 'uncatalyzed' portion of the rate profile corresponding to a simple rate determining carbon protonation of enolate by water, results.

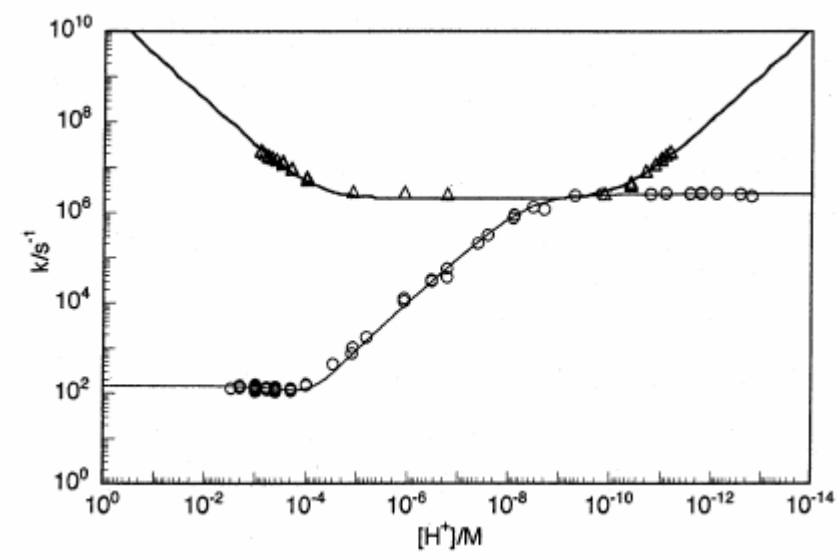

Figure 8: Rate profiles for the hydration of phenylcarbamoylcarbene (△) and ketonization of mandelamide enol (O) in aqueous solution taken from J. AM. CHEM. SOC. 9 VOL. 125, NO. 1, 2003

The pH rate profile measured for the formation of our reaction product 3-hydroxy – oxindole (Figure 9) does not follow a behavior expected for ketonization. The rate constant for the acid catalyzed portion of the profile k_H^+ is around 2 x 10^{10} $M^{-1}s^{-1}$. This is several orders of magnitude higher than a typical value for carbon protonation of the nonionized enol by the hydronium ion.

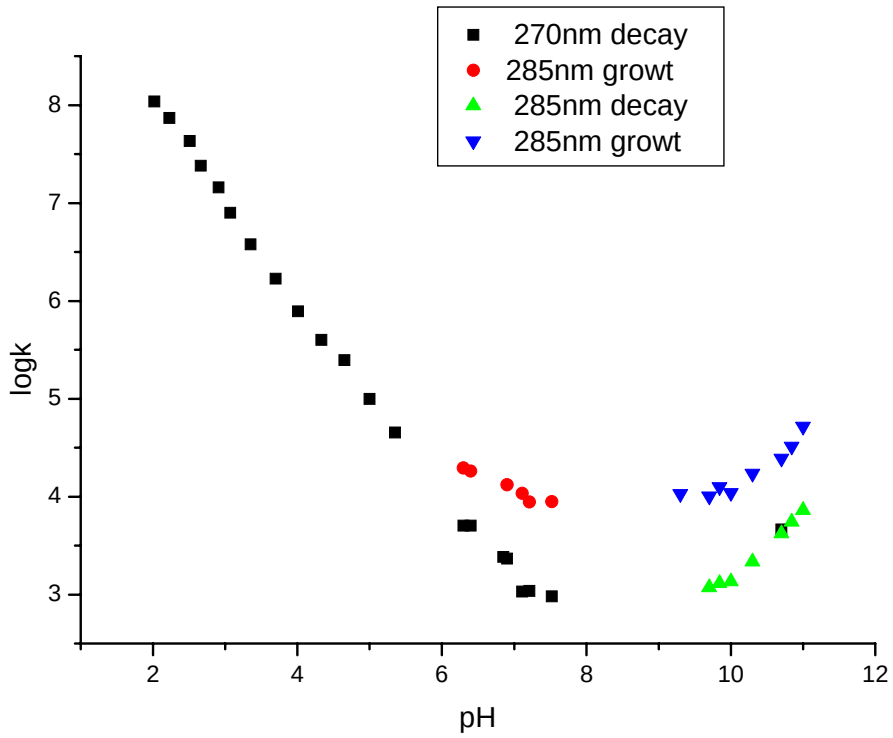

Figure 9: Rate profiles for the processes observed after flash photolysis of 3-diazo-2-indolinone in aqueous solution

Comparison of rates of reaction in H_2O and D_2O gave isotope effects in the normal direction kH/kD =1.14 (Figure 10). However, the value for rate-determining hydron transfer to carbon is expected to be higher. There is no argument based on the structure or other properties of studied compound, which could let us assign our measured pH rate profile to the ketonization of 3-hydroxy – oxindole enol tautomer.

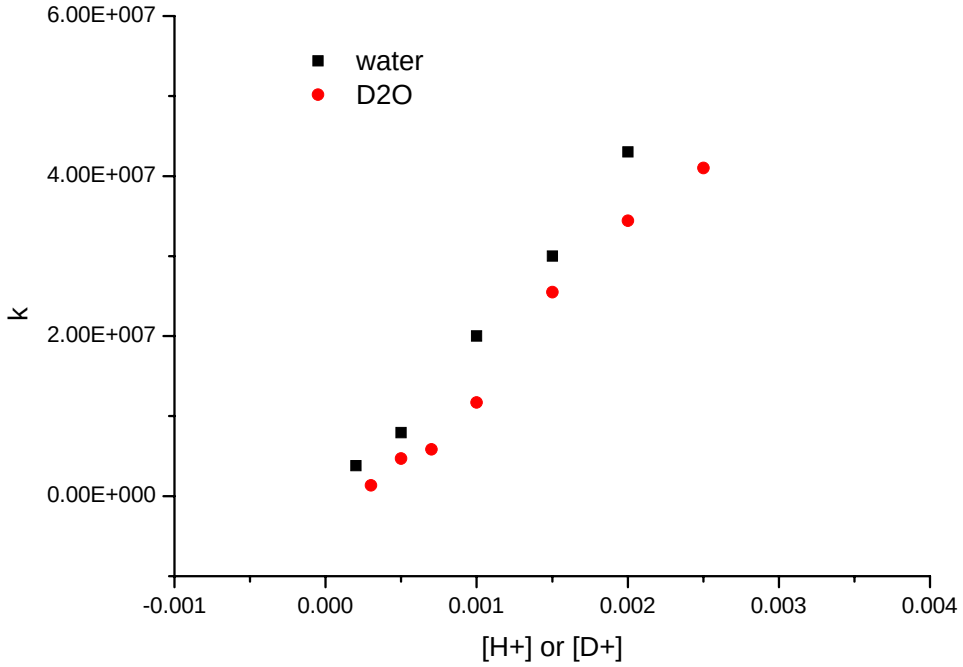

Figure 10: Observed decay rate constants of 270 nm transient in H_2O and D_2O solutions as a function of perchloric acid concentration.

On the other hand, the measured pH rate profile can not be assigned to direct hydration of the carbene either, since the reaction of the carbene with water was observed by the femtosecond pump probe spectroscopy. No subsequent reaction than the one described in the pH profile was detected. The second step of another pathway, which may be taken into account (Figure 7), the nucleophilic attack on the protonated carbene, would not be catalyzed by proton since the concentration of the nucleofile [OH^-] is inversely proportional to [H^+]. This excludes an enol pathway and leaves an ylide formation with subsequent proton transfer. However, there are not many such direct experimental observations of water or alcohol ylides described in literature. More experiment and perhaps calculations will be necessary to support or dismiss this theory.

References

(1) Chapman, O. L.; Chang, C. C.; Kolc, J.; Rosenquist, N. R.; Tomioka, H., Journal of the American Chemical Society, 97(22), 6586-8, **1975**.

(2) Voigt, E., Meier, H., Chemische Berichte, 108(10), 3326-35, **1975**.

(3) Moriconi, E. J., Murray, J. J., Journal of Organic Chemistry, 29(12), 3577-84, **1964**.

(4) Olson, D. R. and M. S. Platz., Journal Of Physical Organic Chemistry 9(11): 759-769, **1996**.

(5) Chiang, Y.; Kresge, A. J.; Tang, Y., S.; Wirz, J., Journal of the American Chemical Society (1984), 106(2), 460-2.

(6) Wirz, J., Pure and Applied Chemistry, 70(11), 2221-2232, **1998**.

(7) Chiang, Y., E. A. Jefferson, et al., Journal Of Physical Organic Chemistry 11(8-9): 610-613, **1998**.

(8) Chiang, Y.; Kresge, A. J.; Schepp, N. P.; Xie, R.-Q., Journal of Organic Chemistry, 65(4), 1175-1180, **2000**.

(9) Chiang, Y., H. X. Guo, et al., Journal Of The American Chemical Society 125(1): 187-194, **2003**.

(10) Schepp, N. P. and J. Wirz, Journal Of The American Chemical Society 116(26): 11749-11753, **1994.**

2.4. Calculations.

Calculations on various levels of theory including high-level G3(MP2)//B3-LYP composite procedure[1] have been used to study cyclic carbene 2-oxindol-3-ylidene **2** as well as all its possible reaction intermediates and transition states connecting these species.

The primary goal of these theoretical investigations was to support or exclude conceivable reaction mechanisms and to predict some characteristics that would be difficult to determine experimentally, for example singlet-triplet splitting of carbonyl carbenes. The singlet-triplet splitting in carbenes has attracted considerable experimental and theoretical attention[2]. Moreover, there have been a number of recent theoretical studies of the S-T splitting including some done on carbonyl carbenes[3,4].

Besides other information obtainable by theoretical investigations, relative energies of comparable species, energetic barriers of the reactions and frequencies of IR, bands were of particular interest. These characteristics can be easily aligned with experiments.

2.4.1 Theoretical Procedures

Ab initio molecular orbital theory and density functional theory calculations were carried out using the Gaussian 98 and Gaussian 03 package of programs[5].

Geometries of stationary points (intermediates and transition states) were optimized using either B3LYP density functional theory or MP2 perturbation theory with the 6-31G(d) basis set. Frequency calculations were done for all stationary points. The connections of the transition states with the reactants in both directions were established by intrinsic reaction path (IRC) calculations. Theoretical calculations performed at this fairly simple level were also used for predictions of infrared spectra. For all the density functional theory calculations, predicted frequencies of infrared bands were scaled with a factor 0.9613.

Zero-point energy (ZPVE) corrections, required to correct raw relative energies at 0 K, were obtained from frequencies calculations. Multilevel G3(MP2) and G3(MP2)//B3LYP methods were selected for very accurate energy calculations.

2.4.2 Results and Discussion

Carbenes have low-lying singlet and triplet states and because their reactivity is state specific, the magnitude of the singlet-triplet (S-T) splitting is of great importance. In a recent theoretical study[4], G3MP2B3 high-level method was found to give reliable results for singlet-triplet energy gaps of α-carbonylcarbenes and for the energy barriers to Wolff-rearrangement.

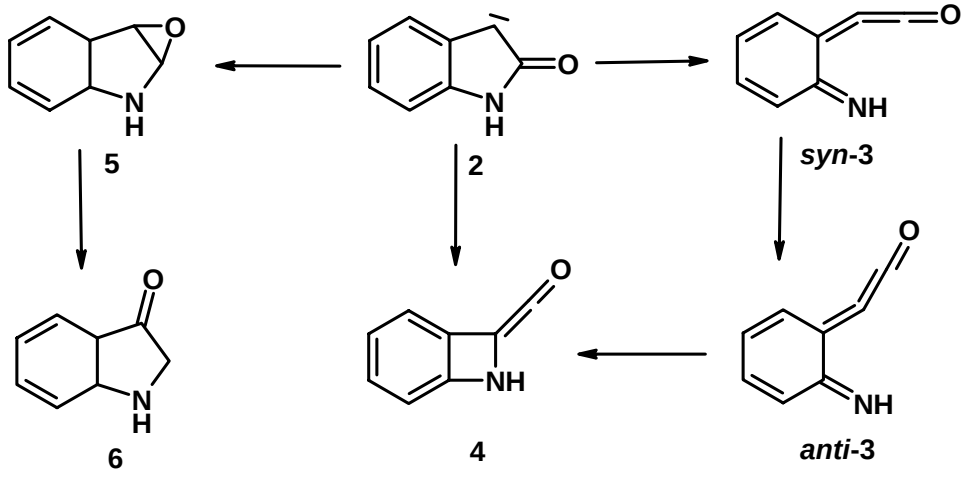

Figure 1: Reaction intermediates included in the ab initio and DFT calculations.

We applied this method as well as conventional B3LYP and MP2 with 6-31G* basis set to examine the ΔE_{ST} and relative energies of species in Table1. Compounds **2-3** were also calculated with the standard G3(MP2) model, which gave very similar results to G3MP2B3. Both of these methods predicted a triplet ground state for carbene **2** and a singlet-triplet energy gap of about 6 kJ mol^{-1}.

However, relative energies predicted for singlet and triplet carbenes by the B3LYP and MP2 methods differed quite substantially. Not surprisingly, high-level methods are required for an adequate treatment of these open shell species. On the other hand, the energies calculated for **3** to **6**, and for the transition states connecting them, showed satisfactory agreement between the four methods.

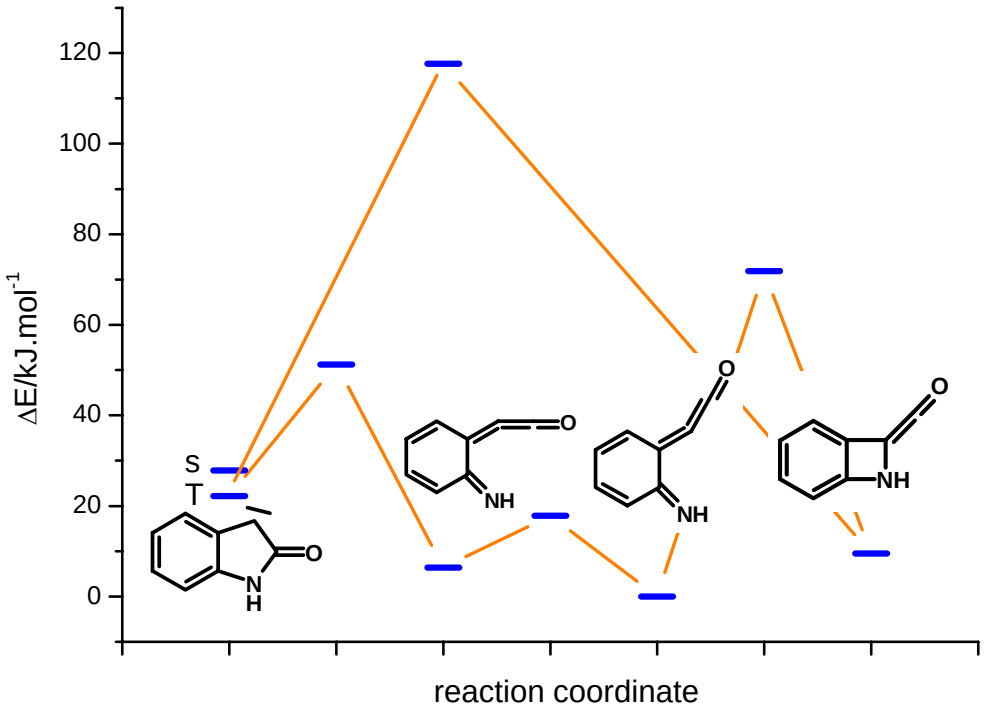

Figure 2: G3(MP2)B3 energies (relative to *anti*-cumulenone **3**, Table 1) of the stationary points connecting **2-4**.

Acyclic carbonyl carbenes have usually triplet ground states with planar geometries and the corresponding singlet carbenes normally adopt a near-orthogonal geometry between the carbonyl and the carbene plane, allowing an overlap between the oxygen lone pair and the formally vacant p orbital at the carbene center[2]. In our cyclic molecule, the carbene is forced to be planar by the geometrical constraints thus preferring triplet state.

stationary points	ΔE [kJ/mol]			
	G3MP2B3	G3MP2	B3LYP/6-31G(d)	MP2/3-31G(d)
^{1}**2**	27.83	23.63	34.18	57.48
^{3}**2**	22.17	17.77	4.05	123.3
syn-**3**	6.36	0	11.65	10.59
anti-**3**	0		0	18.82
4	3.13		0.61	0
^{1}**2** → *syn*-**3**	51.28		66.56	87.46
syn-**3** → *anti*-**3**	17.83		20.63	
^{1}**2** → **4**	117.61		138.41	151.4
anti-**3** → **4**	71.87		130.2	
^{1}**5**				
^{3}**5**			253.88	270.53
6	-63.51		-24.71	
^{1}**2** → **6**			231	

Table 1: Calculated Zero-Point Energies (relative to cumulenone *anti*- **3** and to ketene **4** respectively) of reaction intermediates **2-4** and the transition states connecting them.

The calculated geometry of the cumulenone moiety of **3** is not linear but kinked although the structure keeps its planarity (Figure 3).

The *anti* - geometrical conformation of **3** is 6.3 kJ/mol lower in energy than corresponding *syn* conformer. They are connected via transition state 11 kJ/mol above *syn* structure. The geometry of cumulenone has also an influence on the vibrational spectra. Their CCCO bands are predicted to be 30 cm^{-1} separated (Table 2).

compound	IR band calculated			IR band experimental
^{1}**2**	1605	1755	3484	
^{3}**2**	1670	1572		
anti-**3**	2126			2120
syn-**3**	2094			
4	2134			

Table 2: IR band frequencies calculated on B3LYP/6-31G* level, scaled by factor 0.9613

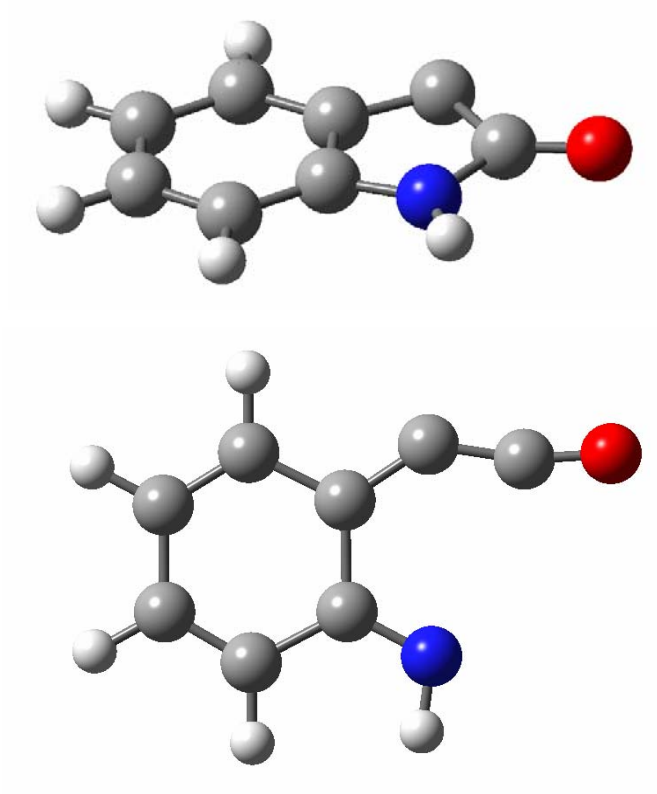

Figure 3: 3D ball and stick model of intermediates **2** and **3**

Expected intermediates of carbonyl carbene **2** isomerization, cumulenone **3** and cyclic ketene **4** lie on very similar energy levels 28 and 25 kJ/mol under singlet carbene that is presumably their precursor. The examination of transition states connecting them revealed their separation from the singlet carbene by substantial energetic barriers 23.5 and 90 $kJmol^{-1}$ respectively. An energetic barrier of 90 kJ/mol is according to Arrhenius equation

$$k = Ae^{-E_a / RT}$$

too high for a reaction taking place in picoseconds time scale. The preexponential factor A would exceed its theoretical limits by about 10 orders of magnitude. Calculated activation energy of 23.5 kJ/mol for the reaction of ^{1}**2** to *syn* **3** together with the

experimentally determined rate constant of 6 x 10^9 s^{-1} yields on the other hand a log A (s^{-1}) = 13.85 at 300K. This appears to be somewhat larger but still reasonable value for an unimolecular rearrangement[5].

We should also take into an account a substantial vibrational energy excess of so-called hot carbene. Typical bond dissociation energies for the carbon nitrogen bond in diazo compounds are 80-120 kcal mol^{-1}, so excitation with a 265 nm photon (435 kcal mol^{-1}) prepares an initial excited state with energy well about the ground state even if most of excess energy appears as kinetic energy of the N_2 photoproduct. Cooling usually requires around 50 ps depending on the solvent[6]. The energetic barrier separating the ground states of carbene and cumulene may thus effectively be less than 23.5 kJ. The *anti* form of cumulenone **3** and cyclic ketene **4** are separated by a transition state that is predicted to be 70 kJ/mol above the level of these intermediates. This barrier rules out any thermal isomerization within upper limit of their expected lifetimes.

α-Carbonylcarbene might also exist in equilibrium with an elusive oxirene[7]. Oxirenes were observed to mediate the interconversion of isomeric carbonyl carbenes (Figure 1). In order to learn more about this possible reaction pathway, we calculated energies of **5-6** and transition state connecting **4** with **6**. We found that singlet oxirene is not an energy minimum on the reaction pathway. It is a transition state, instead. The triplet oxirene was found to be an energy minimum around 230 kJ higher than cumulenone *anti* – **3.** The oxygen atom was predicted to be out of the plane of the rest of the molecule.

Possibility of valence isomerization of diazo group in 3-diazo -2 oxoindoline was discussed in the work of Voigt and Meier[8]. We studied diazo, diazirine and 1,2,3 - Oxadiazole isomers on B3LYP/6-31G* level. The diazo isomer is predicted to be the most stable structure 75 kJ lower in energy than diazirine. The transition state separating both isomers lies 201 kJ/mol above the energy of the diazo compound. The structure corresponding to the oxadiazole was not found to be an energetic minimum.

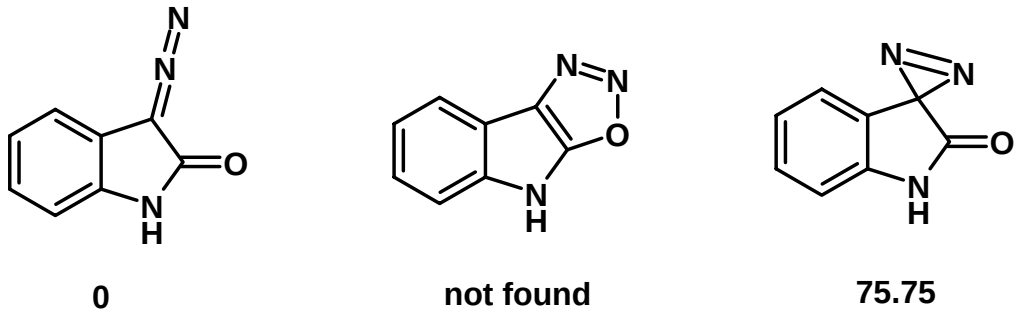

Figure 4: ZPE-corrected energies in kJ mol^{-1} of 3-diazo-2oxoindoline and its valence isomers

References

(1) Baboul, A. G.; Curtiss, L. A.; Redfern, P. C.; Raghavachari, Krishnan., Journal of Chemical Physics, 110(16), 7650-7657, **1999**.

(2) R.A. Moss, M. S. P., M. Jones, Jr., Reactive Intermediate Chemistry. New York, Wiley, **2003.**

(3) Scott, A. P., M. S. Platz, et al.. Journal Of The American Chemical Society 123(25): 6069-6076, **2001**.

(4) Xie, Y.; Schaefer, H. F., III., Molecular Physics, 87(2), **1996**.

(5) Murai, H.; Safarik, I.; Torres, M.; Strausz, Otto P., Journal of the American Chemical Society, 110(4), 1025-32, **1988**.

(6) Hess, G. C., B. Kohler, et al.,. Journal Of The American Chemical Society 122(33): 8087-8088, **2000**.

(7) Lewars, E., Canadian Journal of Chemistry, 78(2), 297-306, **2000**.

(8) Voigt, Erika; Meier, Herbert., 108(10), 3326-35, **1975**.

2.5. Infra Red spectroscopy - step scan experiments

The reaction mechanisms of 3-diazo-2-indolinone have been examined by steady state and time resolved infrared spectroscopy.

Fourier-Transform Infrared (FTIR) spectroscopy is an interferometric method. Therefore, the spectrum is not directly measured but its interferogram, i.e. the IR intensity reaching the detector as a function of the mirror position. The spectrum is subsequently obtained by Fourier transformation of the interferogram from the time domain into the frequency domain. The major advantages of FTIR spectroscopy, as compared to conventional dispersive IR spectroscopy, are the so-called multiplexing advantage and the high energy flux reaching the detector, allowing rapid spectrum acquisition at a high signal to noise ratio.

For time-resolved infrared spectroscopy, a special technique, the step-scan mode was developed[1]. In the classical technique, the temporal change of a sample after e.g. light excitation is examined by recording subsequent spectra. The time resolution in this technique is limited by the scanning speed of the moving mirror and is about 20 milliseconds in the so-called rapid-scan mode. In the step-scan mode, the position of the moving mirror remains fixed at a particular position, and a complete time course of the change of the interferogram evoked by the reaction is recorded at this particular mirror position. This procedure is repeated at all other mirror positions and a 3D represenation of the temporal evolution of the entire interferogram is obtained by combining the respective time traces. Fourier transformation and deduction of the sample steady state spectra yields the corresponding 3D representation of the time evolution of the IR difference spectra.

The step-scan instrument[2,3] was built by the design of Rödig and Siebert using a Bruker IFS 66v/s Fourier transform infrared spectrophotometer equipped with a globar IR source, a KBr beam splitter, a nitrogen-cooled MCT detector and an external DC-coupled preamplifier. Nd:YAG laser (266nm, pulse width 6 ns, pulse energy $\leq$5 mJ, pulse frequency 10 Hz) was used for excitation. The spectral IR region was restricted to 2257–1130 cm^{-1} by using a cut-on/cut-off filter combination. Deuterated acetonitrile solutions

of studied compounds were used with an optical density of 0.2 at the excitation wavelength. The solution was flowed through the sample cell (CaF_2 windows, 200μm path length) to avoid re-irradiation of transient intermediates and photoproducts. The experiments were carried out with a resolution of 8 cm^{-1}. The Fourier-transformed data were baseline corrected and factor analyzed in the region 1300–2200 cm^{-1}. Two significant factors were sufficient to reproduce the time evolution of the spectra within experimental accuracy. This procedure resulted in a substantial elimination of noise and massive data reduction.

2.5.1 Results and discussion

The IR spectrum of 3-diazo-2-indolinone (**1**) exhibits very strong bands (Figure 1) at 2095, and 1695 cm^{-1}, and weaker bands at 1618 1468, 1408, and 1333 cm-1 in CD3CN. Time-resolved IR difference spectra generated by pulsed laser irradiation of **1** at 266 nm in CD3CN exhibited strong negative bands at the positions 2095 and 1695 due to depletion of **1** by the laser flash (Figure 2). The negative bands were formed within the time resolution (50 ns) of the instrument. In addition, a positive absorption band at 2120 cm^{-1} was formed within 50 ns. The decay of this band obeyed a dual exponential kinetics $k_1 \approx 2 \times 10^5$ s^{-1} (Figure 4). Simultaneously a band at 2095 cm^{-1} grew in with the same kinetics (Figure 3).

The transient absorption at 2120 cm^{-1} is in good agreement with the expected[4] and also calculated value 2123 cm^{-1} from B3LYP/6-31G* calculation for cumulenone **3**. In addition, the first rate constant obtained by a global fit of the data corresponds very well to the one measured by laser flash photolysis for 450 nm absorption decay. Thus, the 2120 cm^{-1} band can attributed to the cumulenone **3.**

Step scan experiments in 20% D_2O in CD_3CN solutions have been also done. However, as we already know from laser flash photolysis and the pump - probe experiments there is more than one reaction pathway in wet acetonitrile solutions. Complexity of the time resolved spectra increased to a level that discouraged us from further investigations.

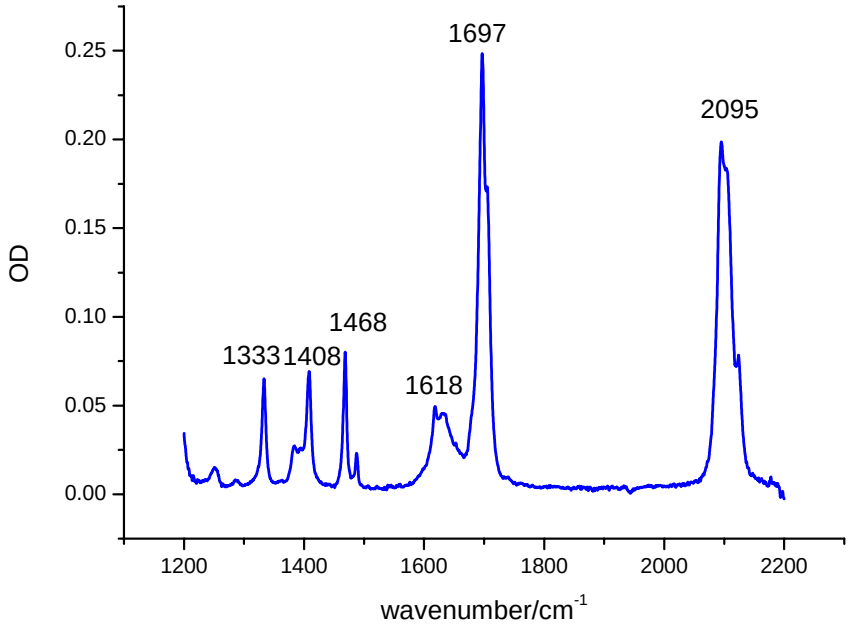

Figure 1: Infra Red spectrum of 3-diazo-2-indolinone in CD_3CN.

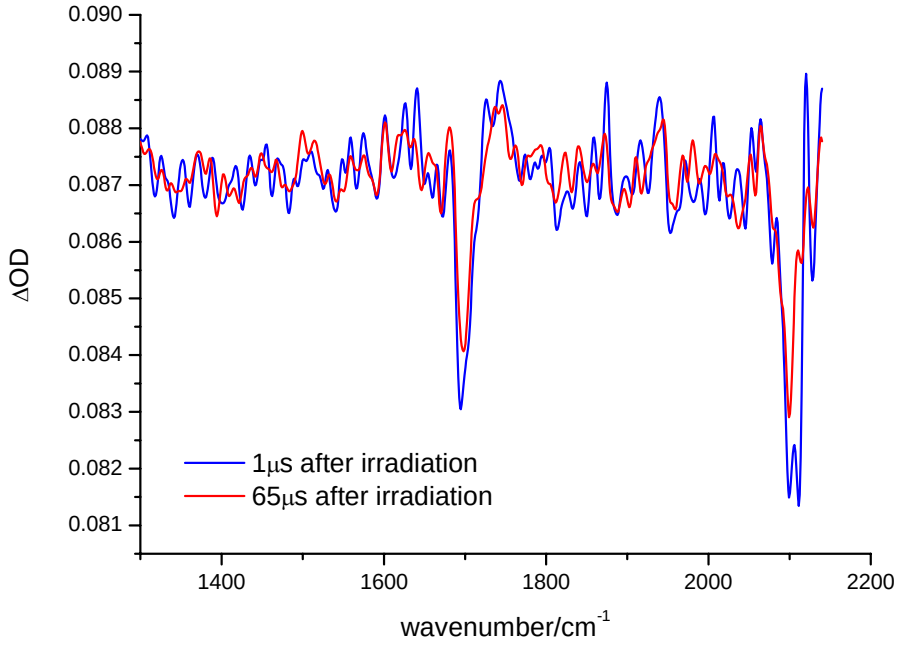

Figure 2: Time resolved IR difference spectra observed in 1300-2200 cm^{-1} spectral region 1 μs and 65 μs after the irradiation of 3-diazo-2-indolinone.

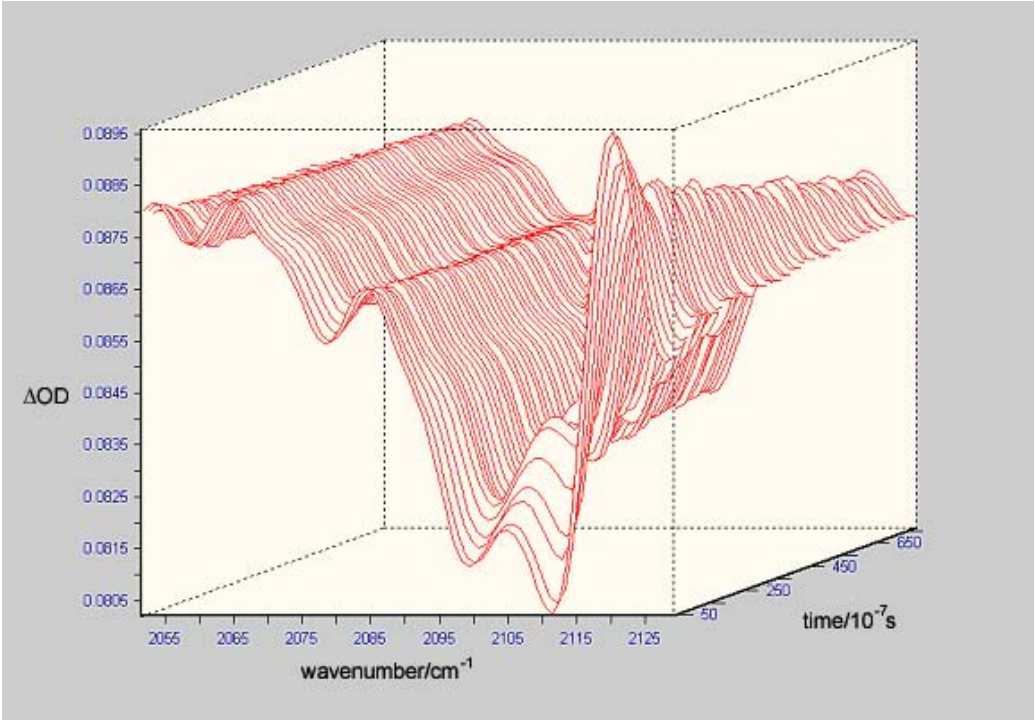

Figure 3: Temporal evolution of the IR difference spectra of 3-diazo-2-indolinone in CD3CN after excitation at 266 nm.

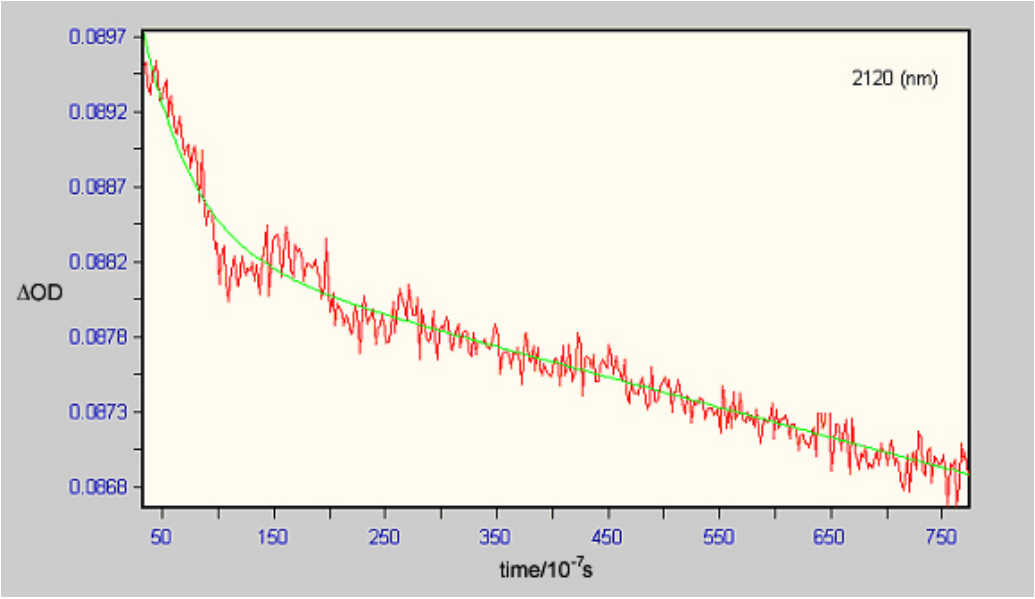

Figure 4: Kinetic trace of the decay at 2120 cm^{-1}, the green line is fit coming from the global analysis of the data.

References

(1) Rödig C, Siebert F Instrumental aspects of time-resolved spectra generated using step-scan interferometers. in: Handbook of Vibrational Spectroscopy, Vol. 1: Theory and Instrumentation. Chalmers JM, Griffiths PR (eds.), John Wiley & Sons, Chichester, UK **2002**.

(2) Rödig C, Siebert F., Appl Spectrosc 53:893-901, **1999**.

(3) Rödig C, Georg H, Siebert F, Rousso I, Sheves M., Laser Chem 19:169-172, **1999.**

(4) Wagner, Brian D.; Zgierski, Marek Z.; Lusztyk, Janusz., Journal of the American Chemical Society, 116(14), 6433-4, **1994**.

3. Summary

The aim of this work was the investigation of 3-diazo-2-indolinone photoreactions as a part of the larger project concerning 1-diazo-2-indanone derivatives[1]. In a recent work, we published data on photochemistry of 3-diazo-3*H*-benzofuran-2-one[2] and the study of 1-diazo-2-indanone is an ongoing project.

The α - carbonyl carbene was identified by ultra fast pump probe spectroscopy experiments as the sole primary photoproduct of 3-diazo-2-indolinone in solution. It is formed within one picosecond upon irradiation. The possibility of rapid equilibration via intersystem crossing with its triplet state was discussed, based on the high-level ab initio calculations. The calculations predict a triplet ground state of studied compound in the gas phase. Ring-opening reaction of a singlet carbene is strongly favored over Wolff rearrangement reaction or oxirane formation by the calculations.

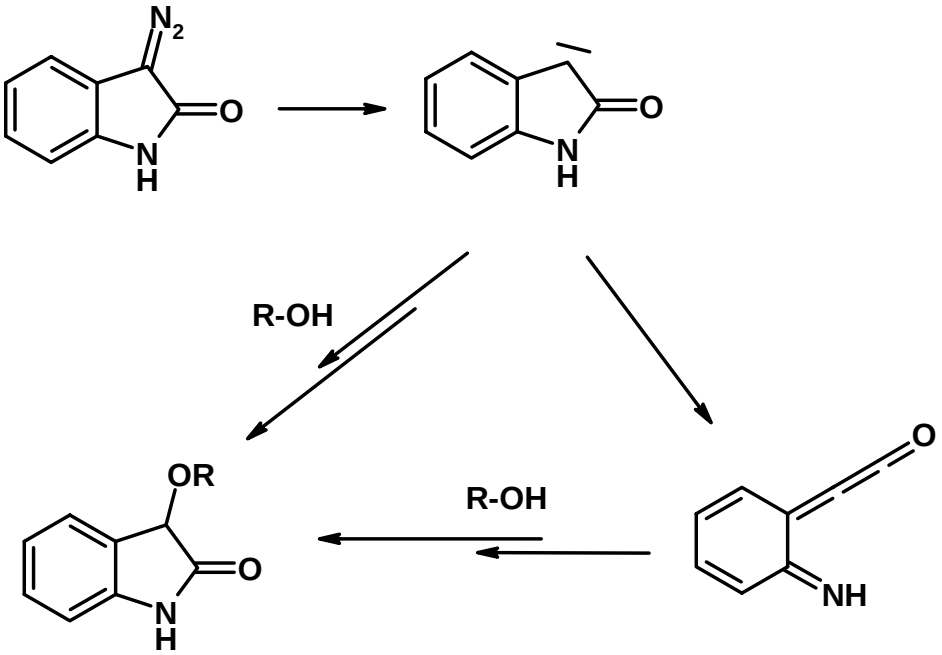

The singlet carbene intermediate undergoes the ring opening reaction, yielding cumulenone in aprotic solvents, $k \approx 5.9 \times 10^{10}$ s^{-1}. The cumulenone structure of the intermediate was confirmed by step scan FTIR measurements in CD_3CN. In aqueous solutions, the primary photoproduct is intercepted by water with a rate of $k_{H2O} \approx 7 \times 10^9$ M^{-1} s^{-1}. The yield of cumulenone is thus reduced with increasing water concentration. 3-

Hydroxy-2-indolinone is the major product isolated after irradiation of 3-diazo-2-indolinone in aqueous solutions. It is formed by two reaction pathways depending on the water concentration in solution. They are either an O-H group insertion into the singlet carbene or alternatively hydration of the cumulenone. The O-H insertion is obviously favoured at higher water concentrations. We studied the mechanism of O-H insertion by laser flash photolysis technique.

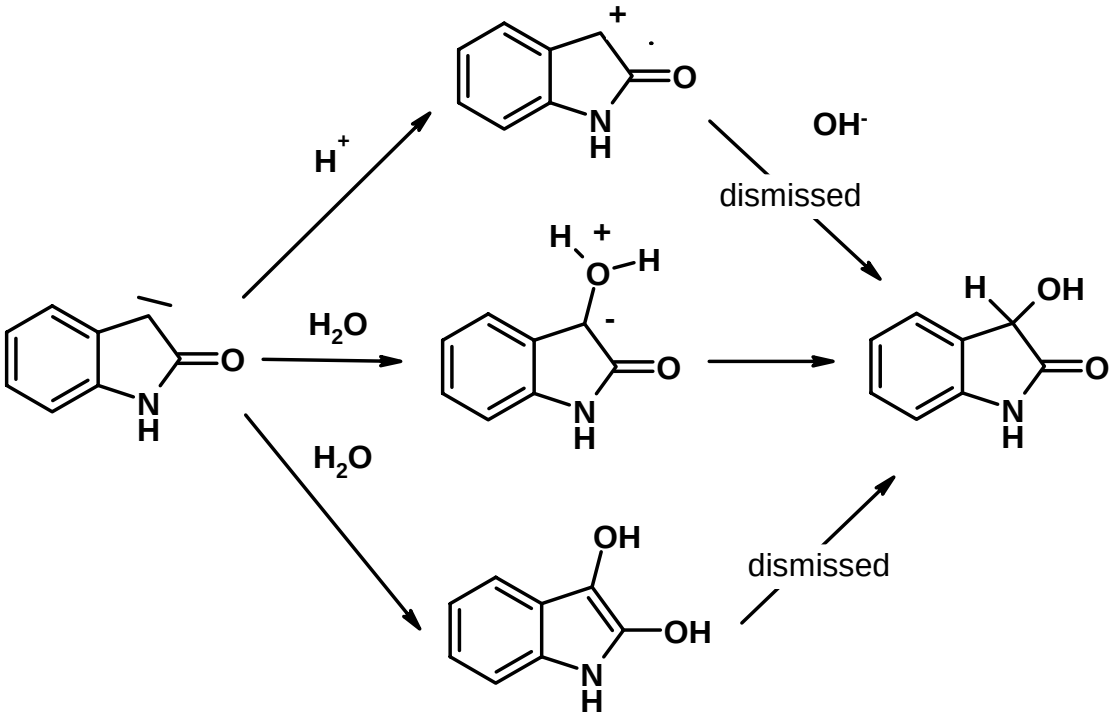

These experiments failed to detect any transient attributable to the enediol intermediate, which would be expected to show similar absorbance at 275 nm and ketonization kinetics as the enol of mandelic acid amide. The lack of such a transient ruled out the enol formation pathways of singlet carbene insertion into an O-H group. The pH rate profile has an acid-catalyzed portion $k_{H^+} \approx 2 \times 10^{10}\ M^{-1}s^{-1}$ followed by a complex uncatalyzed region. This behavior is in contradiction with all known mechanisms except the ylide formation followed by the proton transfer. This would suggest a long-lived ylide intermediate. Such a structure has not been observed yet. Therefore, for the complete understanding of the O-H insertion mechanism some additional experiments are necessary.

The second goal of this work was the construction of the femtosecond pump-probe spectroscopy setup. The constructed setup allows the direct spectroscopic observation of the ultra short-lived intermediates in the wavelength range from 300 to 700 nm. The time resolution achieved is around 180 fs. The repetition rate of the setup is 426 Hz and the time resolved spectra can be measured within 1.8 ns time window.

Other projects, in which I have been involved during my PhD study, were the investigation of photochemical reaction mechanisms of 2-nitrobenzyl compounds[3], the study of an excited state intramolecular proton transfer in 2-naphtol and the study of energy and electron transfer in various Porphyrin - Deazaflavin systems.

(1) Gaplovsky M., Boudebous H., Wirz J.,Versatile Carbenes from 1-Diazo-indan-2-one Derivatives, 7th International Conference on Reaction Mechanisms, Dublin July, 2004

(2) Chiang, Y., M. Gaplovsky, et al. "Photoreactions of 3-diazo-3H-benzofuran-2-one; Dimerization and hydrolysis of its primary photoproduct, a quinonoid cumulenone: A study by time-resolved optical and infrared spectroscopy." Journal of The American Chemical Society 125(42): 12872-12880, 2003.

(3) M. Gaplovsky, Y. V. Ilichev, Y. Kamdzhilov, S. V. Kombarova, M. Mac, M. A. Schwörer and J. Wirz, Photochemical reaction mechanisms of 2-nitrobenzyl compounds: 2-Nitrobenzyl alcohols form 2-nitroso hydrates by dual proton transfer. Journal of Photochemical and Photobiological sciences, accepted

4. Curriculum Vitae

Personal Data:

Name	Martin Gáplovský
Date of birth	February 26, 1977
Nationality	Slovak

Education

2001-2004	PhD study at the department of physical chemistry, University Basel, in the group of Prof. J. Wirz.
2000-2001	PharmDr. theses at Pharmaceutical Faculty of Comenius University, Bratislava, Department of medicinal chemistry: *Molecular modeling of 5-Lipoxygenase inhibitors.* Group of Prof. M. Remko
1995-2000	MSc. study at Pharmaceutical Faculty of Comenius University Bratislava. Diploma thesis at department of medicinal chemistry: *Molecular modeling of some beta-adrenergic inhibitors* Group of Prof. M. Remko
1998-2001	Undergraduate research at Institute of Chemistry, Comenius University Bratislava. *Ultrasound effect on photochemical reactions*.

During my studies at University of Basel I attended lectures by:

J Wirz, E. Dangel - Pelloquin, J. Seelig, A Vedani

5. Appendix